

## Design of Oil and Air Squeeze Film Dampers For a Ball Bearing Turbocharger

*Edgar J. Gunter, PhD*

*Prof. Emeritus of Mech. and Aerospace Engineering, Univ. of Virginia*

*Former Dir. Rotor-Bearing Dynamics Laboratory*

*Fellow ASME*

### **ABSTRACT**

*This paper examines the stability and dynamic characteristics of a high speed ball bearing turbocharger supported by an uncentered oil squeeze film damper cartridge as compared to the dynamical characteristics of a turbocharger with a closed-end air squeeze film damper system. The concept of an air squeeze film damper is not new as they been employed since the 1960s in high-speed dental drills.*

*The standard turbocharger bearings used in both diesel and automotive engines have been the floating ring bearing design. These floating ring bearings are inexpensive to produce, but turbochargers with floating ring bearings have an inherent stability problem. The floating ring bearing was originally developed in the 1930s by General Motors as a way of reducing bearing friction losses. A plain journal bearing, for example, would be unstable at speeds above 8,000 RPM. Obviously a plain journal bearing is unsuitable for use in a turbocharger running in the range of 100,000 RPM and above.*

*Turbochargers in floating bush bearings are inherently unstable and are in a constant state of subsynchronous whirling, exciting either the first or second turbocharger critical speeds. However, these turbochargers are able to operate successfully because they have controlled limit cycle whirl motion due to the bearing nonlinear stiffness effects. Additional instability driving forces acting on the turbocharger are also present. These unstable forces are the Alford cross-coupling forces generated on the compressor and turbine impellers, particularly at high power levels.*

*An advanced generation of turbochargers has been developed using rolling element bearings. Rolling element bearings inherently do not suffer the instability problems encountered with floating bush bearings. However, rolling element bearings have fundamental problems in that they lack the damping to control the instability generated by the Alford forces and also to provide the necessary damping required to pass through the two critical speed regions. The rolling element bearing turborotors, therefore, require some form of a damper system. For example, all aircraft engines use squeeze film dampers with centering springs. The current design of ball bearing turbochargers employs an uncentered squeeze film bearing-damper cartridge with narrow damper lands and tight damper clearances. With an uncentered oil squeeze film damper, it is difficult to optimize both the stiffness and damping characteristics of these turbochargers.*

*There is another fundamental problem that is encountered with ball bearing turbochargers with uncentered oil squeeze film dampers, and that is the occurrence of **damper lockup**. This situation occurs with moderate to high levels of unbalance. Under conditions of moderate or high unbalance, mass center phase inversion does not occur due to excessive compressor damper stiffness. The compressor amplitude continues to increase while attempting to pass through the second critical speed region until volute rubbing occurs. This results in a violent backward rotor whirling, leading to shaft failure.*

*The use of closed-end air squeeze film dampers has several significant advantages. The first obvious one is that no fluid is required to supply the damper. The second advantage is that no radial stiffness is generated from the air damper. The stiffness of the damper system is determined by the design of the O-ring grooves and the O-ring material. The stiffness properties of the rubber O-rings are only mildly nonlinear. Thus, damper lockup does not occur with turbochargers provided with centered air squeeze film dampers.*

*The use of centered air squeeze film dampers represents a significant improvement in stability and reliability over the current use of uncentered oil squeeze film dampers. It is anticipated that the next generation of these turbochargers will employ air squeeze film dampers.*

## Resume

### *Edgar J. Gunter, PhD*

Dr. Gunter is a Professor Emeritus of Mechanical and Aerospace Engineering at the University of Virginia. He received his Mechanical Engineering degree from Duke University and Masters and PhD degrees from the University of Pennsylvania in Engineering Mechanics.

He was employed as a centrifugal compressor design engineer for four years at Clark Brothers, Olean, New York, now a division of Dresser-Rand. Based on his compressor design projects, he was awarded a National Defense Fellowship to pursue the PhD degree in Engineering Mechanics.

During his graduate studies, he received an internship with the SKF Ball Bearing Research Center to study the fatigue life of rolling element bearings. In his graduate program, he majored in applied mechanics, vibration and dynamics, fluid mechanics and lubrication theory.

After completing his formal training at the University of Pennsylvania, he assumed the position of Senior Research Scientist at the Franklin Institute Friction and Lubrication Laboratories and was in charge of research in the Gas Bearing Division. While at the Franklin Institute, he received a NASA Lewis Research Center Grant to study rotor-bearing stability. The study was initiated since at that time the Franklin Institute had some of the world's largest digital and analog computers. The report on Rotor Bearing Stability was published by NASA as a special CR report and received national distribution. This report formed the basis of his PhD dissertation.

Upon receiving his formal PhD degree, Dr. Gunter was then offered the position of Associate Professor of Mechanical and Aerospace Engineering at the University of Virginia. At the University, he developed the Rotor-Bearing Dynamics Laboratory to assist industry in the development of reliable high-speed rotating equipment.

In 1999 Dr. Gunter formed the software and consulting company, RODYN Vibration Analysis Inc., for consulting services in the field of rotor-bearing dynamics. RODYN is the principal distributor of the rotor-bearing dynamics software *Dyrobex*, developed by Dr. Wen Jeng Chen of *Eigen Technologies*. This software is in use by the major turbomachinery manufactures in U.S. and abroad.

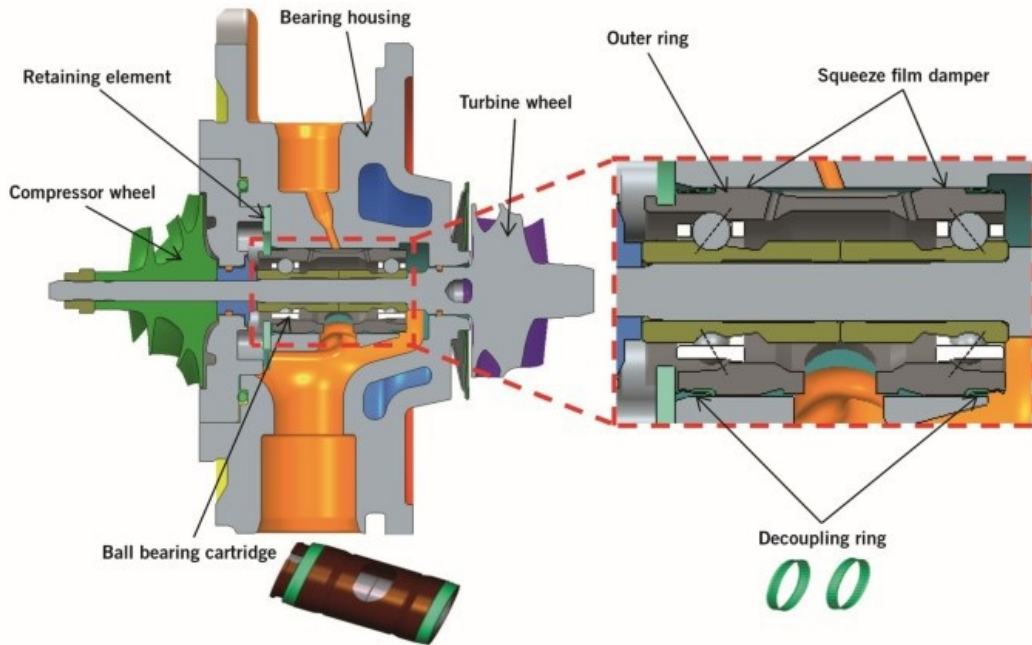
Dr. Gunter's current research is on the dynamics of high speed turbochargers for applications in the field of automotive and large marine diesel engines. He has written numerous papers on the subject of the dynamics of high speed turbochargers and squeeze film dampers for aerospace applications. Additional papers on the subject of rotor-bearing dynamics by Dr. Gunter and other researchers may be found on the company website, [www.RODYN.com](http://www.RODYN.com)

He has been elected to the following honorary engineering societies Pi Tau Sigma, Tau Beta Pi and Sigma Xi. He has been elected a Fellow of ASME.

In 2007, Dr. Wen Jeng Chen and Dr. Gunter published the textbook entitled *Introduction To Dynamics of Rotor Bearing Systems*. This reference book is currently being used as a textbook in both undergraduate and graduate courses in rotor-bearing dynamics, both here and abroad.

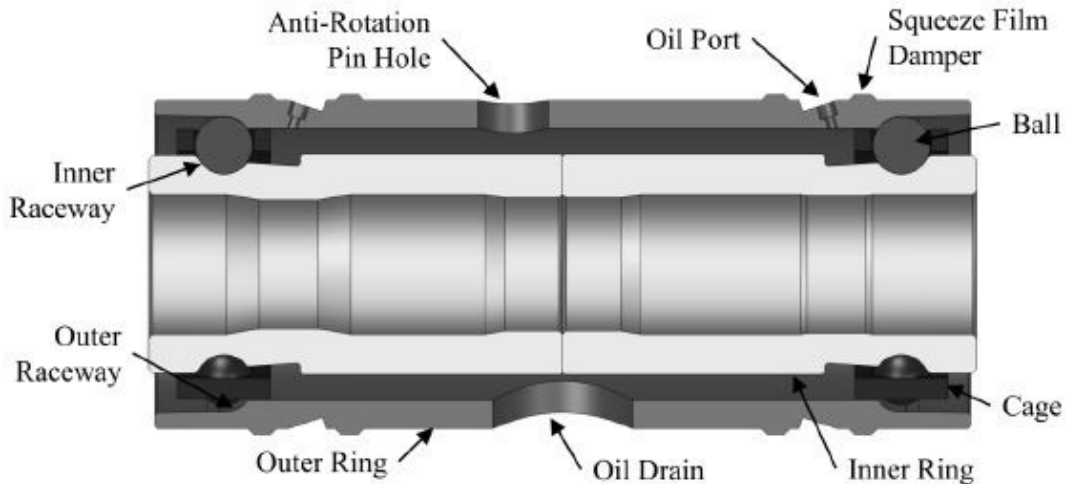
Dr. Gunter was awarded the first Jack Frarey Memorial Metal by the Vibration Institute for contributions to the field of rotor-bearing dynamics in 2008.





**Figure 1.2 Ball Bearing Turbocharger With Oil Squeeze Film Damper**

Figure 1.2 represents a typical ball bearing turbocharger with an uncentered oil squeeze film damper system. The two oil squeeze film dampers are open ended and the damper cartridge is free floating. The damper lands are approximately 0.25 in with a nominal radial clearance of 1 mil. At start up, the damper cartridge is resting on the casing. There is no centering spring used with these damper designs, unlike what is installed with ball bearing dampers for aircraft engines.



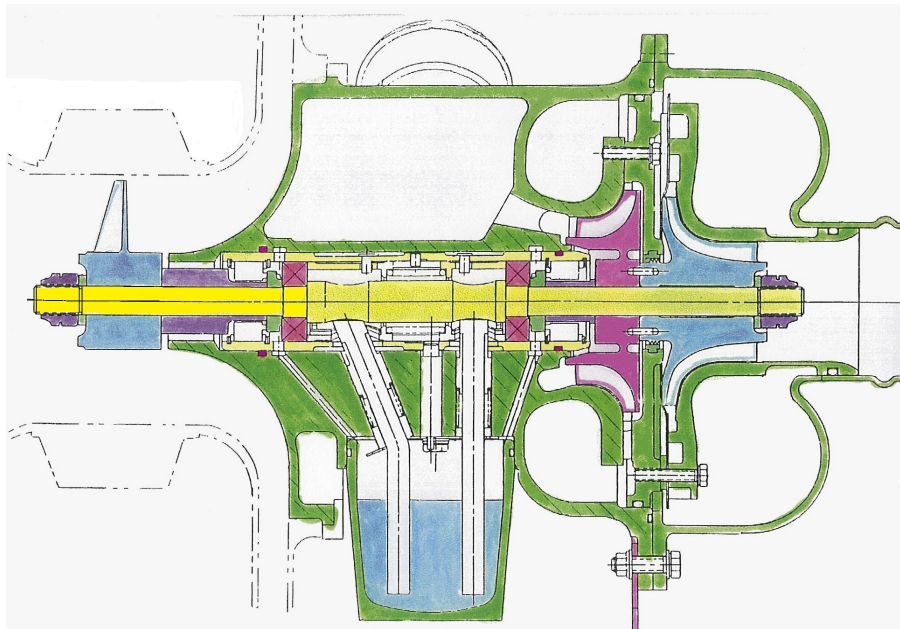
**Figure 1.3 Diagram of Oil Squeeze Film Damper Cartridge**

Figure 1.3 represents a typical free floating oil squeeze film damper system employed on ball bearing turbochargers. Notice the very narrow damper lands used on these damper cartridges. If the turbocharger weight causes these dampers to bottom out or operate at high eccentricities, then the damper system will not be effective. This condition is referred to as ***Damper Lock Up***.



**Figure 1.4 Ball Bearing Cartridge Assembly**

Figure 1.4 shows a typical uncentered ball bearing cartridge. The ball bearing life with this turbocharger bearing-cartridge assembly may be quite limited, since the damper design is not optimal, as it is not a centered damper. The damper can be operating at a high eccentricity ratio to start due to gravity loading.



**Figure 1.5 Aircraft Ball Bearing ACM Unit**

Figure 1.5 represents an HS ACM unit that had been installed on a Cessna Citation Seven aircraft. With aircraft air cycle machines (ACM units), fluid film oil squeeze film dampers cannot be installed as compared with a jet engine. As such as the bearing design for these units is either an air foil bearing or rolling element bearings mounted in a cartridge support.



**Figure 1.6 Bearing Cartridge From Failed ACM Unit**

Figure 1.6 represents the bearing cartridge from the failed aircraft ACM turborotor. The bearing cartridge has one O-ring for centering. The wear tracks caused by the rolling element bearings can be clearly seen on the bearing cartridge particularly the track shown on the right side of the cartridge which corresponds to the compressor side bearing.



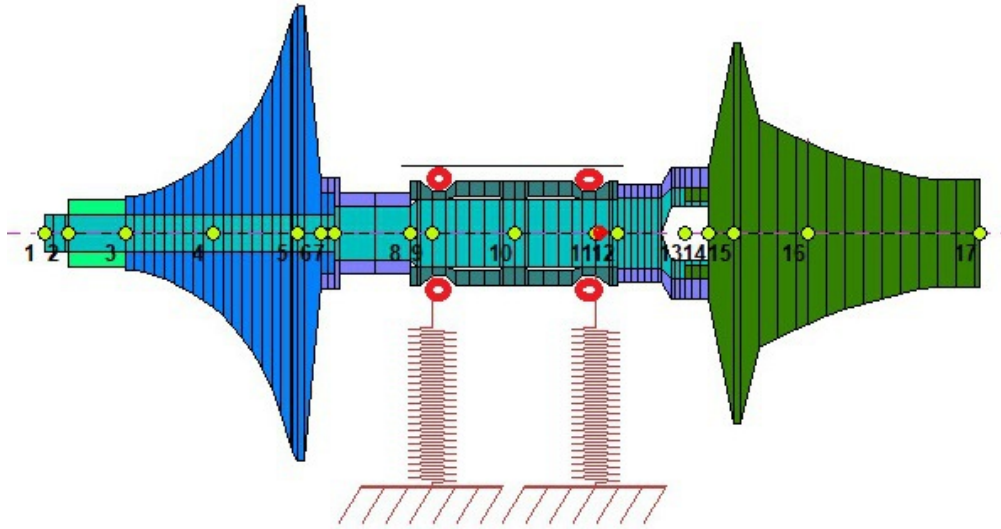
**Figure 1.7 Failed ACM Compressor Impeller**

Figure 1.7 represents the failed ACM compressor impeller. The single O-ring that was installed on the damper cartridge did not provide for an adequate damper system. As a result of the large whirling of the ACM unit, the compressor rotor was severely impacted, destroying the impeller blades. It was reported that these ACM aircraft units were failing in as little as 3 to 6 months.

The cartridge was redesigned to incorporate two air squeeze film dampers to provide system damping. The design of air squeeze film dampers will be discussed in detail in a later section. Four closely fitting O-rings were used to seal the two air damper chambers. The air squeeze film damper concept has several advantages over an oil squeeze film damper for smaller high-speed turbine rotors. One obvious advantage is that a lubricating fluid is not required for an air damper, as the damper system is self contained. The inherent stiffness of the damper is provided by the compressed O-rings. Hence the occurrence of damper lockup due to an overloaded damper is not encountered with an air squeeze film damper. The incorporation of the air squeeze film damper proved to be highly successful with the elimination of further bearing failures in this particular ACM unit.

## 2 Turbocharger Critical Speed Analysis on Rigid and Flexible Supports

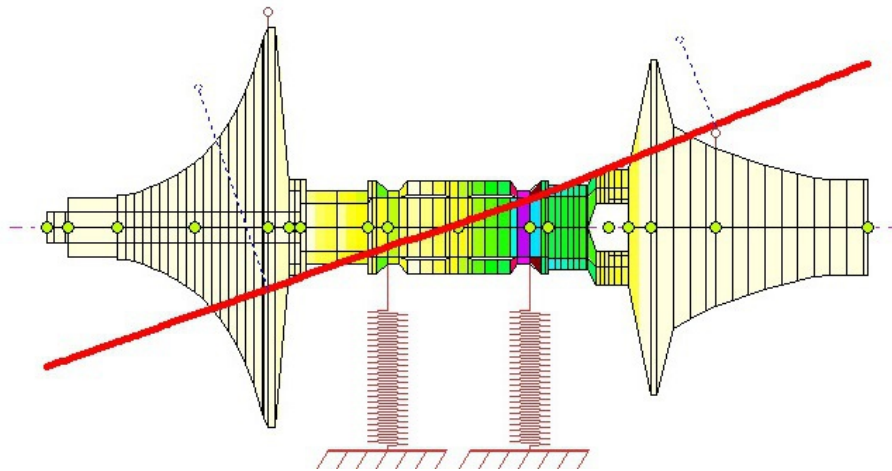
### Critical Speeds on Rigid Supports



**Figure 2.1 Turbocharger With Rolling Element Bearings on Rigid Supports**

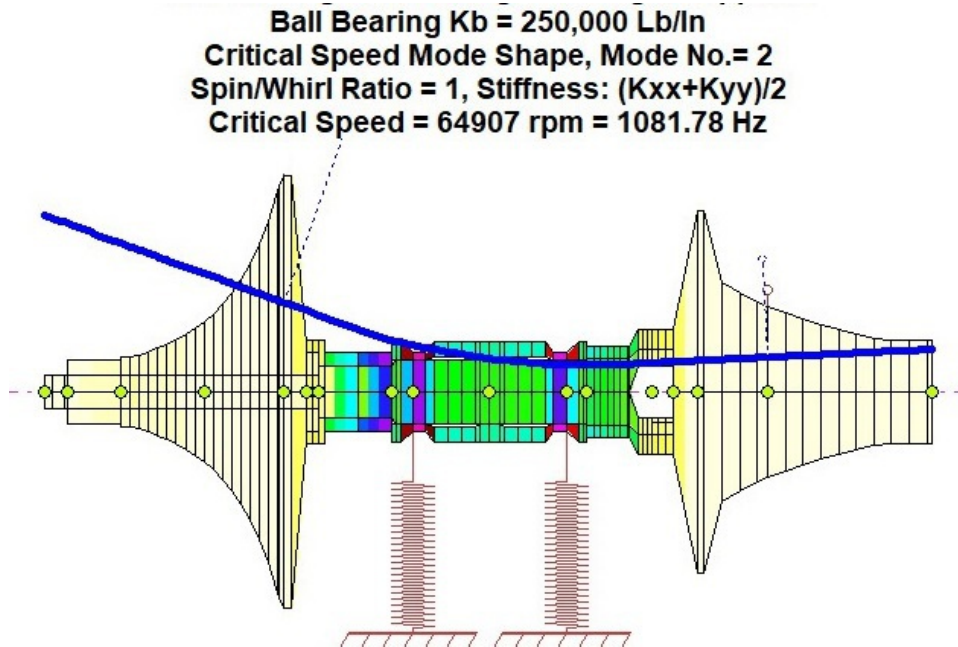
Figure 2.1 represents the turbocharger mounted on rigid supports. The first step in evaluating the turbocharger is to compute the turbocharger critical speeds with the rolling element bearings rigidly supported. In this case the rolling element bearing stiffness is assumed to be 250,000 lb/in.

**Ball Bearing Turbocharger on Rigid Supports**  
**Ball Bearing  $K_b = 250,000 \text{ Lb/in}$**   
**Critical Speed Mode Shape, Mode No.= 1**  
**Spin/Whirl Ratio = 1, Stiffness:  $(K_{xx}+K_{yy})/2$**   
**Critical Speed = 24123 rpm = 402.04 Hz**



**Figure 2.2 Turbocharger 1<sup>st</sup> Critical Speed On Rigid Supports**

Figure 2.2 represents the turbocharger first critical speed at 24,123 CPM with the rolling element bearings on rigid supports. In this case it is seen that the first critical speed is a rigid body conical mode in which the strain energy is situated in the bearings. The motion of the compressor and turbine are out of phase with very little strain energy in shaft bending. This first critical speed is controlled by the inherent stiffness of the bearing support system. It will be seen that when a flexible system support is added, the first critical speed will be reduced.



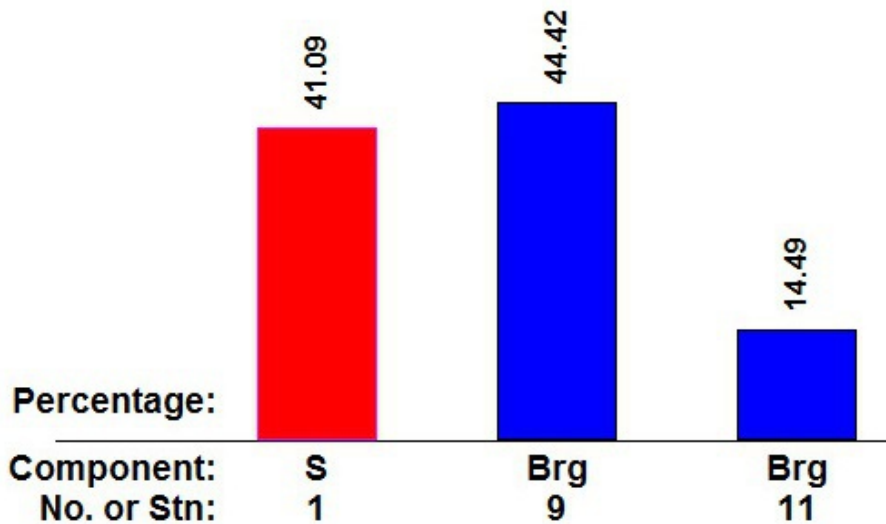
**Figure 2.3 Turbocharger 2nd Critical Speed On Rigid Supports**

Figure 2.3 represents the turbocharger second critical speed on rigid supports. In this case the second critical speed is at approximately 65,000 CPM with considerable shaft bending through the bearing section and significant motion at the compressor. Note that the motion of the turbine and compressor are in phase.

**Mode No.= 2, Critical Speed = 64907 rpm = 1081.78 Hz**

**Potential Energy Distribution (s/w=1)**

**Overall: Shaft(S)= 41.09%, Bearing(Brg)= 58.91%**



**Figure 2.4 2nd Critical Speed Energy Distribution**

Figure 2.4 shows that in the 2<sup>nd</sup> mode, 44% of the system strain energy is in the compressor end bearing, with only 14% energy in the turbine bearing. Note that the first mode is a rigid body mode with all of the strain energy in the bearings. In this mode, there is considerable shaft bending with 41% strain energy in shaft bending.

With double overhung turborotors, it is desirable to avoid the third critical speed which involves considerable shaft bending and low bearing damping.

## Critical Speeds on Rigid Supports

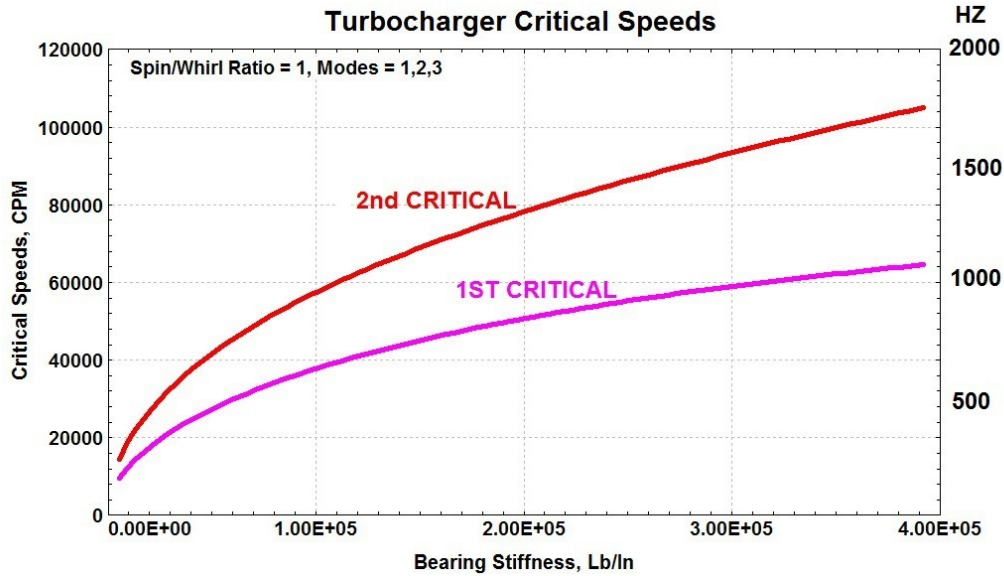


**Figure 2.5 Turbocharger Critical Speed Map**

Figure 2.5 represents the turbocharger first two critical speeds as a function of direct bearing stiffness. The third mode is not shown as it is above the rotor maximum speed of 150,000 RPM. One may assume if subsynchronous whirling is observed in the range of 500 Hz or below then it is whirling in the first mode. This would be the predominant whirl mode that would be expected for this turbocharger.

## Critical Speeds on Flexible Supports

**Ball Bearing Turbocharger Undamped Critical Speeds**  
 Kbrg = 250,000 Lb/In, Kdamper - 10,000 Lb/In  
 Critical Speed Mode Shape, Mode No.= 1  
 Spin/Whirl Ratios = 1, 0, Stiffness:  $(K_{xx}+K_{yy})/2$   
 Critical Speed = 4958 rpm = 82.63 Hz

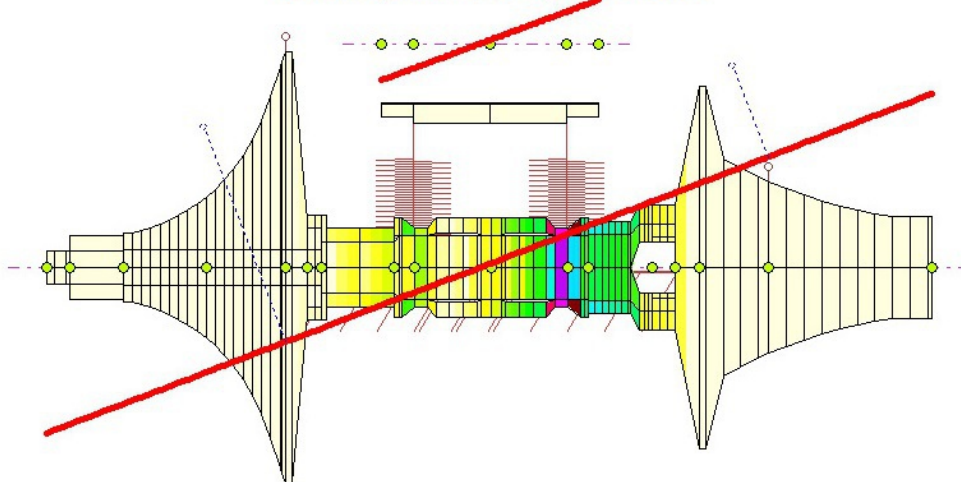
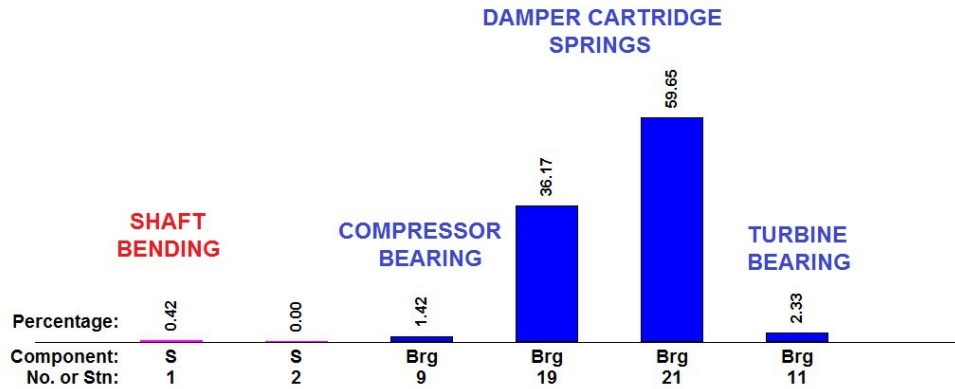


**Figure 2.6 Turbocharger 1st Critical Speed With Damper Cartridge**

Figure 2.6 shows the turbocharger first critical speed at approximately five thousand RPM with the damper cartridge with an assumed spring rate of 10,000 Lb/In. The value of damper cartridge effective spring rate of 10,000 lb/in +/- 3,000 lb/in was chosen as it was determined to an optimum value for this particular turbocharger.

A value of 5,000 lb/in was found to be too soft, and 20,000 lb/in as too stiff. Detailed analysis of optimum linear damper support stiffness and damping K and C will be presented in the next section.

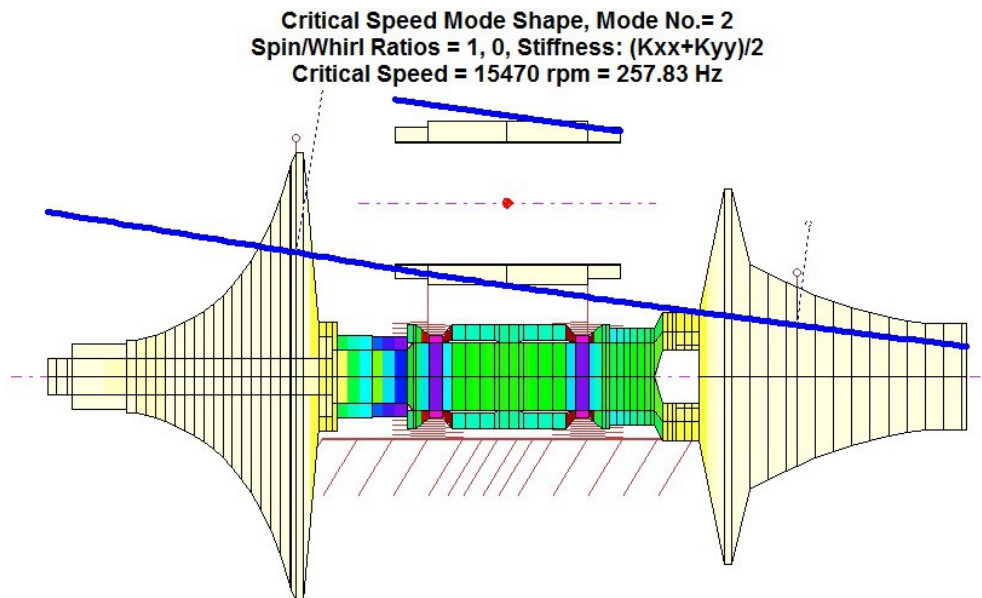
Mode No.= 1, Critical Speed = 4958 rpm = 82.63 Hz  
 Potential Energy Distribution (s/w=1)  
 Overall: Shaft(S)= 0.42%, Bearing(Brg)= 99.58%



**Figure 2.7 1<sup>st</sup> Mode Shaft and Bearings Strain Energy Distribution**

Figure 2.7 represents the strain energy distribution of the shaft and the rolling element and damper bearing spring rates. It is of particular interest to notice that the strain energy of the rolling element bearings are only 1.4% and 2.3% of the total system energy. Therefore, the exact stiffness of the rolling element bearings is of little importance as there is very little strain energy in the main bearings for this first conical rigid body mode.

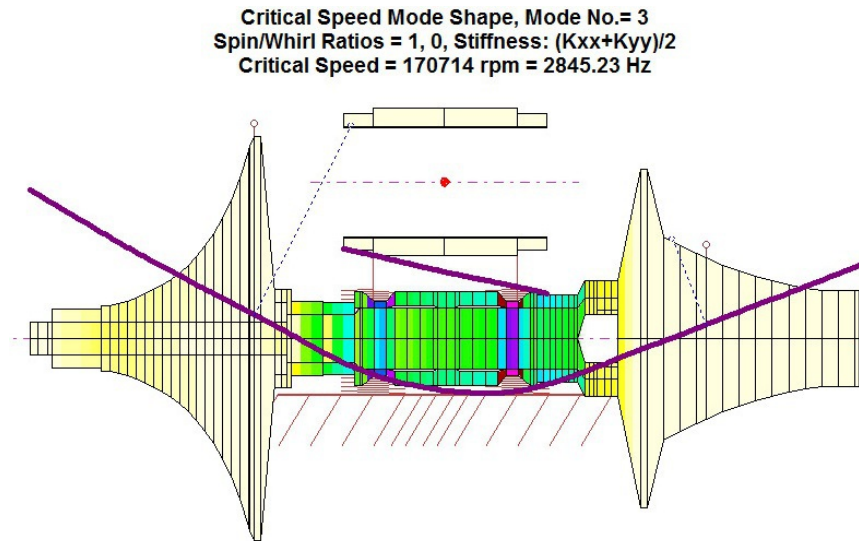
Figure 2.7 also shows that the mode shape is basically a rigid body mode with essentially no strain energy of bending in the shaft. This a very important consideration when performing nonlinear time transient analysis. It is therefore not necessary to have an extensive number of shaft elements in order to accurately compute the transient rotor response under whirl conditions.



**Figure 2.8 Turbochargers 2<sup>nd</sup> Critical Speed at 15,470 RPM**

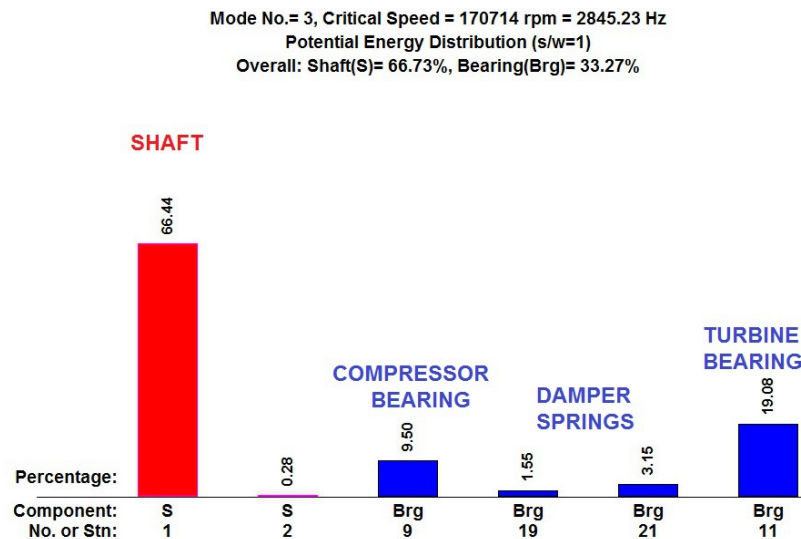
## Critical Speeds on Flexible Supports

Figure 2.8 represents the turbocharger second critical speed at 15,470 RPM on the flexible support system. The second mode is also essentially a rigid body mode with the maximum system strain energy predominantly in the compressor end bearing. The motion at the compressor and turbine are in phase with the maximum amplitude of motion at the compressor location.



**Figure 2.9 Turbocharger 3<sup>rd</sup> Critical Speed**

Figure 2.9 represents the turbocharger third critical speed at 170,714 RPM. The particular design speed for this turbocharger was 150,000 RPM. As can be seen from the rotor mode shaped, there is a considerable amount of bending that takes place with this particular mode. This is the mode that normally limits the top speed of a particular turbocharger, as one should not be operating the turbocharger in this speed range. The reason for this is that the damper bearing system is not a very effective in damping out the 3<sup>rd</sup> bending mode.



**Figure 2.10 Turbocharger 3rd Mode Strain Energy**

Figure 2.10 represents a turbocharger third mode strain energy. As can be seen from Figure 2.10, there is very little strain energy in the damper bearings. Over two-thirds of the strain energy is in shaft bending and 30% in the rolling element bearings. Thus the damper cartridge will be ineffective in suppressing vibration in the third critical speed.

### 3 Ball Bearing Turbocharger Stability and Unbalance Response With Linear Damper Support

#### 3.1 Turbocharger Stability Analysis With Aerodynamic Cross Coupling

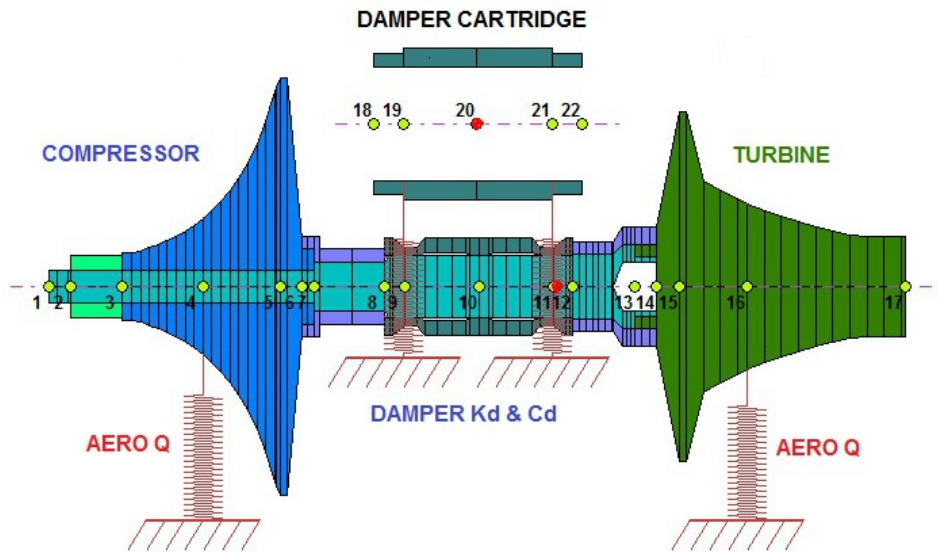


**Figure 3.1 Turbocharger With Aerodynamic Excitation**

Figure 3.1 represents the rolling element bearing with a squeeze film damper. Included in this rotor model is aerodynamic excitation acting on both the compressor and turbine impellers. The aerodynamic cross coupling  $Q$  is expressed as bearing terms of  $K_{xy}$  and  $K_{yx} = -K_{xy}$ .

In order to generate an accurate damper system for the turbocharger, whether it be for an oil squeeze film damper or a captured air damper, it is necessary to understand the optimal values of stiffness and damping that is desirable for this particular turbocharger design.

The turbocharger design is assumed to have a maximum operational speed of 150,000 RPM. The aerodynamic cross coupling is assumed to have values of 500 to 1,000 lb/in acting on both the compressor and turbine impellers. Therefore, before one should embark on a nonlinear time transient dynamical analysis, it should first be determined the range of optimal range of stiffness and damping values that will best promote stability.

The stability analysis for a linear system is a complex eigenvalue analysis in which stability is determined by the value of the log decrement of a forward whirl mode. A negative value of log decrement indicates that the system is unstable and will be subjected to subsynchronous whirling. The whirl motion encountered will normally be associated with the lowest natural frequency of the turborotor. For double overhung turbochargers, this mode is normally a conical whirl mode in which the compressor and turbine motions are out of phase. However it is also possible to excite the second critical speed mode as well under certain conditions.

The object of the stability analysis is thus to determine, for a given stated value of aerodynamic cross coupling  $Q$ , what combinations of support stiffness and damping would promote stability. It should also be noted that if the log decrement for a particular whirl mode exceeds 3.14, then this mode will be critically damped and will not be excited by unbalance.

## Turbocharger Stability For Various Support Stiffness and Damping Values, Kd & Cd

In order to properly design a nonlinear oil or air squeeze film damper system, it is first necessary to perform a linear stability analysis to determine the proper ranges of stiffness and damping that will lead to acceptable stability levels.

Table 3.1, as shown below, represents the log decrement computed for the turbocharger with an aerodynamic excitation cross coupling of  $Q = 1,000 \text{ Lb/In}$ . The log decrement has been computed for a wide range of support stiffness and damping values.

As can be seen in Table 3.1, for a given value of support damping, the log decrement reduces with increase of stiffness for a given damping. This implies, therefore, that as the support stiffness increases, the damping in the support becomes less effective. This table, in effect explains the occurrence of “*damper lockup*” with oil squeeze film dampers, as shall be discussed in more detail later. As the orbital motion of an oil squeeze film damper increases, the stiffness increases at a much greater rate than does the damping leading to the condition referred to as damper lockup.

It has been determined that when the damper orbital eccentricity exceeds 50% of the damper clearance, then the generated radial stiffness of the oil squeeze film damper becomes excessive, leading to the condition of damper lockup. When this occurs, the rotor that may become unstable due to the aerodynamic excitation of the compressor and turbine impellers. Thus, the turbocharger in an oil squeeze film damper with low levels of unbalance may be stable, but become unstable with an increase in unbalance due to the nonlinear increase of the stiffness in an oil squeeze film damper system.

It will be seen that this is not the case with an air squeeze film damper. It has determined that there is sufficient damping provided by the enclosed air squeeze film damper, then this nonlinear radial stiffness effect does not exist. The characteristics of an air squeeze film damper is such that, although the damping is small compared to the oil squeeze film damper, it remains fairly constant over a wide eccentricity range and does not develop the radial stiffness of an oil squeeze film damper. If an air damper has sufficient damping to be in use in a turbocharger, its characteristics are far superior to that which can be obtained from an oil squeeze film damper system.

**Table 3.1 Turbocharger Stability For Values of Support Damping And Stiffness**

Cd Lb-S/In	Kd 5,000 Lb/In	10,000 Lb/In	20,000 Lb/In	50,000 Lb/In
<b>1</b>	<i>(Under Damped)</i>	<b>-0.200</b>	<b>-0.198</b>	<b>-0.237</b>
<b>2</b>	<b>-0.126</b>	<b>0.020</b>	<b>-0.055</b>	<b>-0.186</b>
<b>3</b>	<b>0.053</b>	<b>0.234</b>	<b>0.083</b>	<b>-0.136</b>
<b>5</b>	<b>0.363</b>	<b>0.340</b>	<b>0.034</b>	<b>-0.036</b>
<b>10</b>	<b>0.761</b>	<b>0.707</b>	<b>0.710</b>	<b>0.202</b>
<b>15</b>	<b>1.031</b>	<b>0.863</b>	<b>0.863</b>	<b>0.422</b>
<b>20</b>	<b>1.35</b>	<b>1.072</b>	<b>1.072</b>	<b>0.624</b>
<b>50</b>	<b>2.19</b>	<b>2.19</b>	<b>2.19</b>	<b>1.53</b>
<b>100</b>	<i>(Over Damped)</i>	<b>1.31</b>	<b>1.30</b>	<b>1.23</b>

## Turbocharger Damped First Forward Mode

Ball Bearing Turbocharger With Aero Cross Coupling - 1000 Lb/In  
 Kbrg = 250,000 Lb/In, Kdamper - 5,000 Lb/In, Cd - 5 Lb-S/In  
 Mode No.= 4 STABLE : Rotor: 1 FORWARD : Rotor: 2 FORWARD Precession  
 Shaft Rotational Speeds = 150000, 0 rpm  
 Whirl Speed (Damped Natural Freq.) = 19386 rpm (323 Hz), Log. Dec. = 0.3628

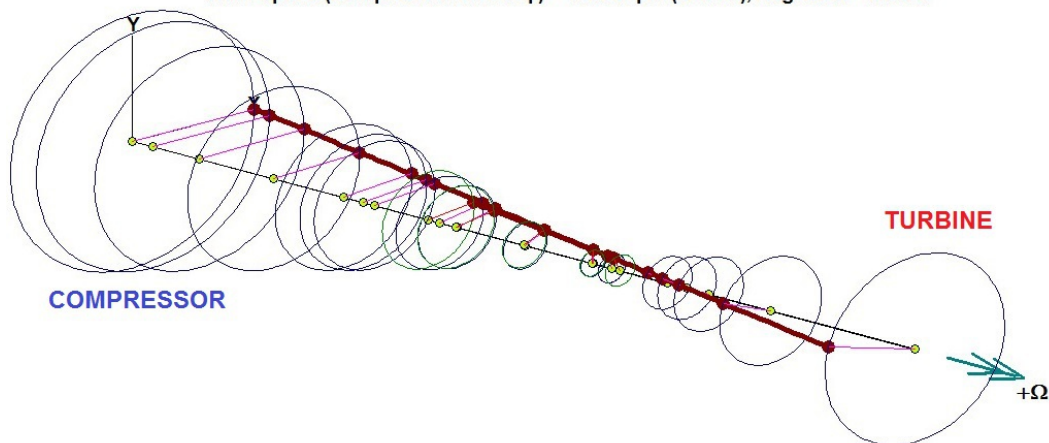


**Figure 3.2 Stable Turbocharger With Support  $K_d = 5,000$  Lb/In  
 $L_d = 0.363$ ,  $C_d = 5$  Lb-S/In, Aero  $Q = 1,000$  Lb/In**

Figure 3.2 represents the first forward mode of the turbocharger with a support stiffness of 5,000 Lb/In. With a damping of 5 Lb-S/In the turbocharger is stable with an  $L_d$  of 0.363. This value of log decrement translates into an unbalance response amplification factor of approximately 8.7 at the first forward critical speed of approximately 20,000 RPM (330Hz). Note that the mode shape is conical with the largest amplitude at the compressor location. This is very typical for turbo compressors in which the turbine impeller is heavier than the compressor. This can be seen from Figure 3.1 which shows that the center of gravity is exactly situated at the turbine end bearing.

Ball Bearing Turbocharger With Aero Cross Coupling - 1000 Lb/In  
 Kbrg = 250,000 Lb/In, Kdamper - 50,000 Lb/In, Cd - 5 Lb-S/In  
 Mode No.= 2 UNSTABLE : Rotor: 1 FORWARD : Rotor: 2 FORWARD Precession  
 Shaft Rotational Speeds = 150000, 0 rpm  
 Whirl Speed (Damped Natural Freq.) = 20272 rpm (338 Hz), Log. Dec. = -0.0358

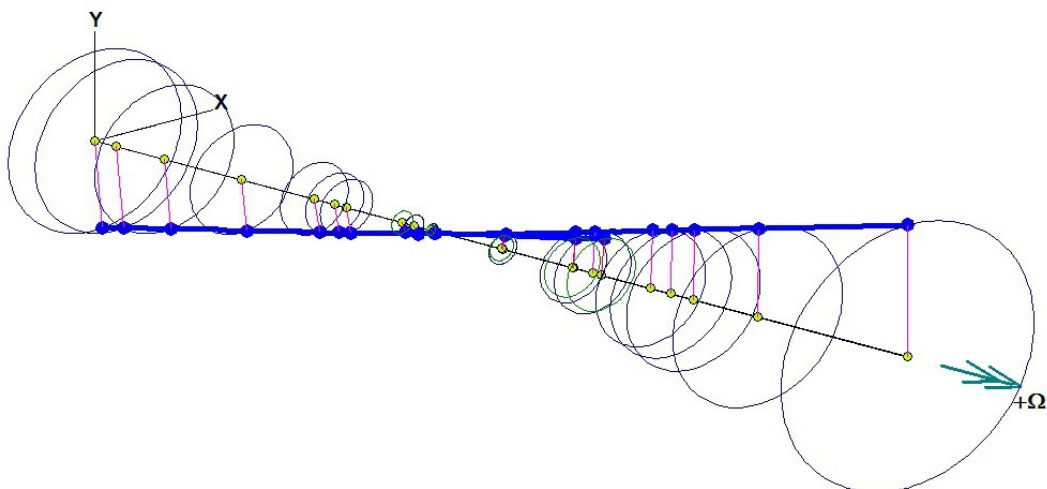


**Figure 3.3 Unstable Turbocharger With Support  $K_d = 50,000$  Lb/In  
 $L_d = -0.036$ ,  $C_d = 5$  Lb-S/In, Aero  $Q = 1,000$  Lb/In**

Figure 3.3 shows that when the turbocharger support stiffness is increased to 50,000 lb/in the system is unstable.

## Turbocharger Response For Various Support Stiffness and Damping Values, Kd & Cd

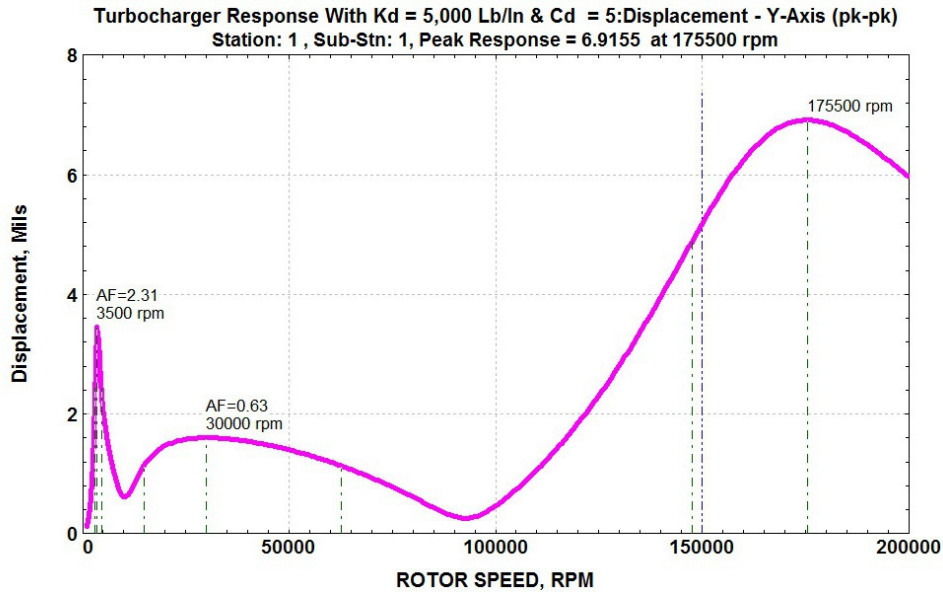


**Figure 3.4 Turbo Response at Compressor With Kd = 5,000 Lb/In And Cd = 5 Lb-S/In, Ub = 0.01 Oz-In**

Figure 3.4 represents the turbocharger response with the damper cartridge having an assumed stiffness value of 5,000 lb/in and the damping a value of Cd = 5 lb-s/in. An unbalance value of 0.01 Oz-In was assumed to be acting at both the compressor and impeller locations. The unbalance situated at the turbine was assumed to be at a 90° position from the compressor unbalance. By this means both the 1<sup>st</sup> and 2<sup>nd</sup> critical speeds should be excited by the unbalance.

Important to note is that at the third critical speed, which is primarily a free-free bending mode, the damping cartridge loses its effectiveness. Thus, it is highly recommended not to operate the turbocharger in the third critical speed range

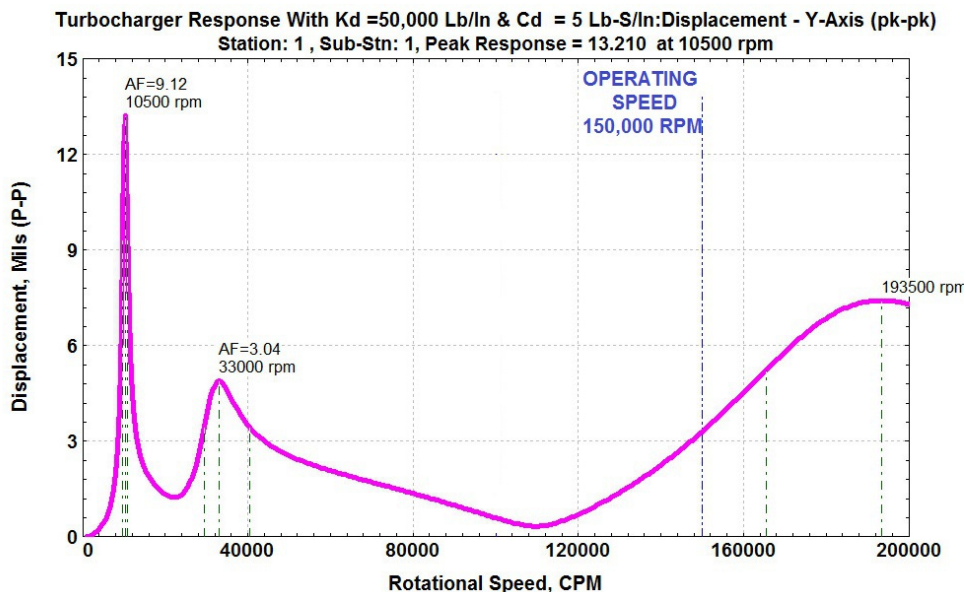


**Figure 3.5 Turbo Response at Compressor With Kd = 50,000 Lb/In And Cd = 5 Lb-S/In, Ub = 0.01 Oz-In**

## Turbocharger Unbalance Response

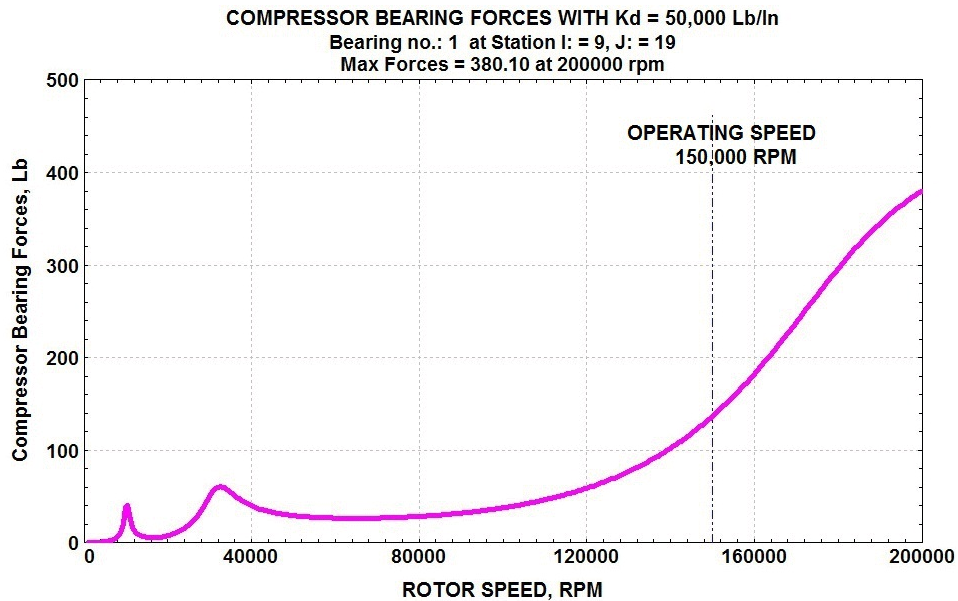


**Figure 3.6 Compressor End Bearing Forces**

Figure 3.6 represents the compressor end bearing forces transmitted with the support spring rate increased to 50,000 lb/in. The forces transmitted at the first and second critical speed are reasonable. As the speed increases, the compressor end bearing forces continue to increase. It is clear that the design speed of this rotor should be restricted to the 150,000 RPM speed range. This particular turbocharger should not be allowed to over speed to the 200,000 RPM range.

As rotor speed increases above the 180,000 RPM range, the third critical speed is encountered. This third critical speed is basically a free-free mode in which there is very little strain energy in the damper bearings. Hence, high amplitudes of motion may occur, as well as high bearing forces. If it is desirable to have a turbocharger that operates in the 200,000 RPM range, then the only acceptable way to accomplish this is by increasing the shaft diameter.

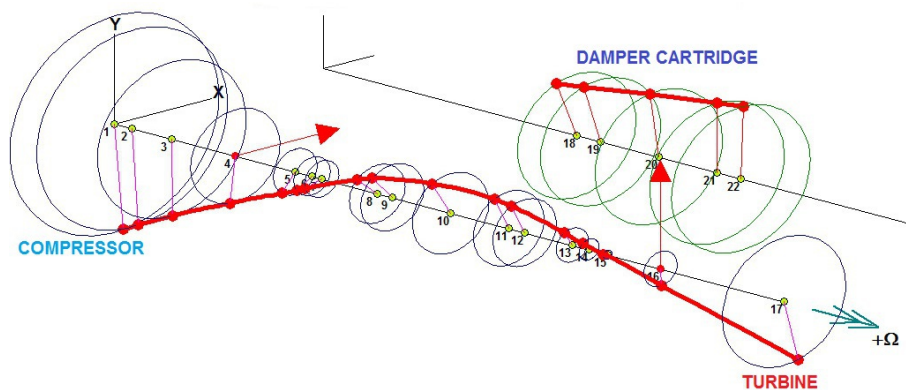


**Figure 3.7 Turbocharger Mode Shape At 200,000 RPM**

Figure 3.7 represents the turbocharger mode shape at 200,000 RPM. It is seen that the largest amplitude of motion occurs at the compressor location. If this mode is encountered and the compressor wheel should contact the volute, then it will proceed in a violent backward whirl mode. This will result in a torsional shaft failure at the turbine impeller.

## 4 Nonlinear Dynamics of A Turbocharger in an Uncentered Oil Film Damper

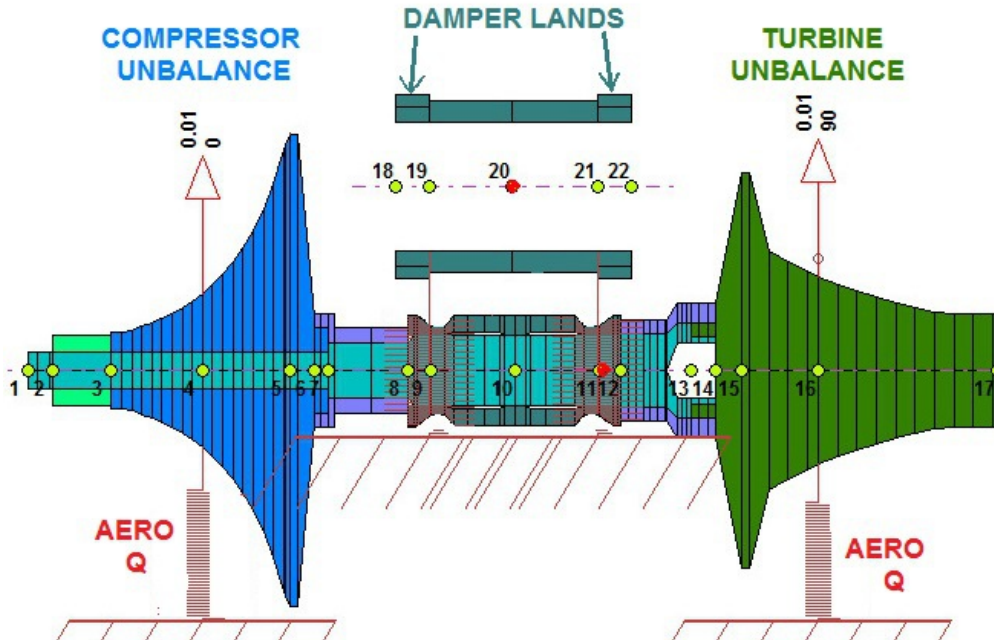


**Figure 4.1 Turbocharger With an Uncentered Oil Film Damper**

Figure 4.1 represents a model of a turbocharger with an uncentered oil squeeze film damper. In addition, the model includes unbalance applied at both the compressor and turbine impellers. In the first model to be evaluated, the unbalance is 0.001 Oz-In. The unbalance at the turbine is placed at a 90° phase angle to the compressor in order to excite both rotor critical speed modes. In addition, aerodynamic excitation of 1,000 Lb/In is assumed acting on both the compressor and turbine impellers to initiate rotor instability.

Axial Forces	Static Loads	Constraints	Misalignments	Shaft Bow	Time Forcing	Harmonics	Base Motion	Torsional/Axial
Units/Description	Material	Shaft Elements	Disks	Unbalance	Bearings	Supports	Foundation	User's Elements

Bearing: 2 of 6  Founder

Station I:  J:

Type:

Comment:

**Damper Properties**

Journal/Damper Diameter:  Axial Length:

Radial Clearance:  Oil Viscosity:

Damper Model:

**Centering Spring Properties**

Stiffness:  Damping:

Unit: (2) - Geometry: in, Viscosity: Reyn (Lbf-s/in<sup>2</sup>), K: Lbf/in, C: Lbf-s/in

**Figure 4.2 Specification of Nonlinear Oil Squeeze Film Damper**

Figure 4.2 represents the specifications for the nonlinear oil squeeze film dampers on the cartridge. As can be seen from the chart, the squeeze film damper has a length of 0.25 in, a radial clearance of 0.001 in and an oil viscosity of 1.0e-6 Reyns. The damper type selected is based on an open ended short bearing assumption with a cavitated Pi pressure profile. Additional information on open and closed squeezed film dampers will be presented in Section 5 on the use of closed end air squeeze film dampers that have a full pressure profile.

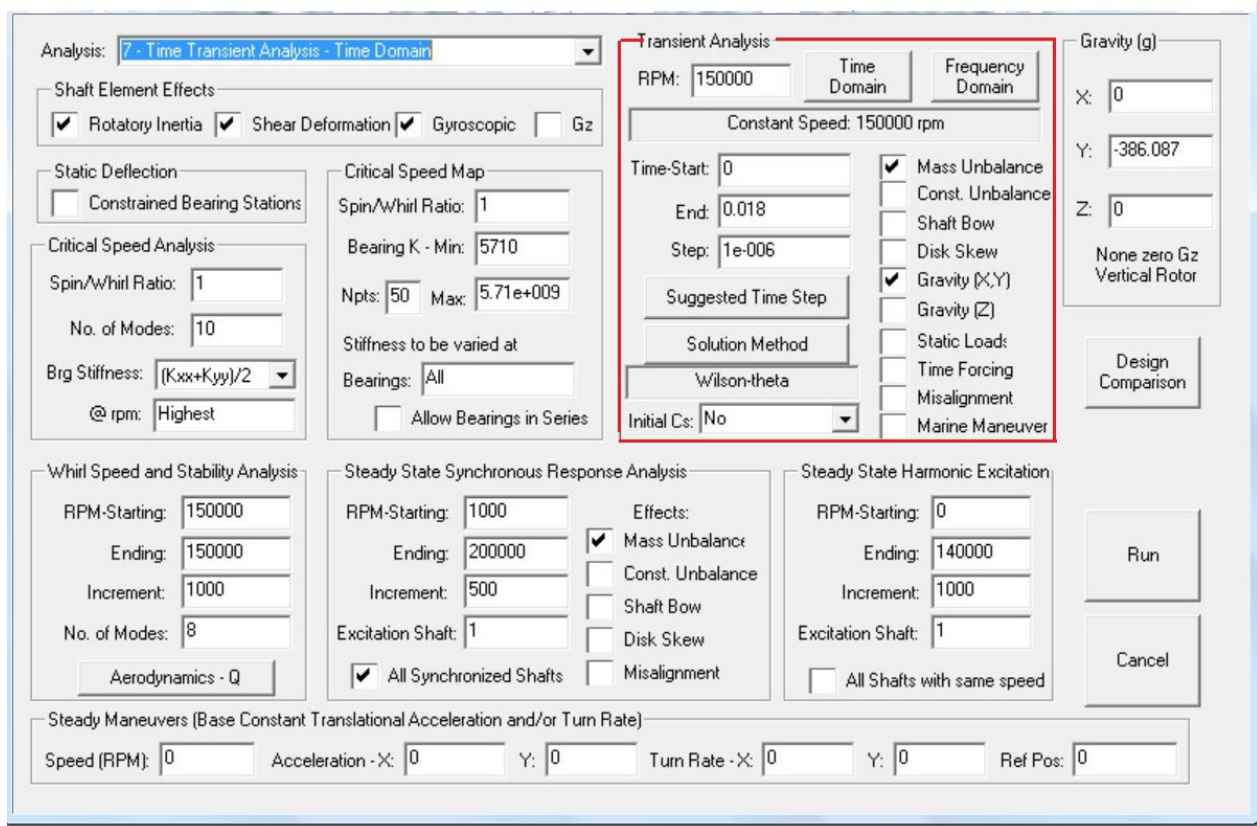


**Figure 4.3 Dyrobes Rotor Dynamic Analysis Options**

In a time transient analysis, many factors may be taken into consideration such as shaft bow, gravitational effects, externally specified loads, as well as other factors as shown in Figure 4.3. The equations of motion of the system are integrated forward in time by one of the numerical methods presented in Dyrobes.

As can be seen from Figure 4.3, the Wilson theta method has been chosen for the numerical integration. Careful consideration must be given to the chosen time step. The rotor is operating at an assumed speed of 150,000 RPM. The time for one revolution of motion is thus  $T_{cycle} = 4.0e-4 \text{ Sec/Cycle}$ . To compute 1 cycle of shaft motion, it will be assumed to utilize 400 steps/cycle, which requires a  $dT$  step of 1.0e-6 sec. With linear systems, a fewer number of steps needs to be taken.

A final time of  $T_f$  of 0.018 sec was chosen. This translates into 45 cycles of shaft motion. In the initial transient motion, there will be a sudden drop in the response of the turbocharger due to the application of gravity. This effect can be ignored by plotting out the motion from 20 to 40 cycles of motion.

When dealing with nonlinear systems, it is often necessary to use a very small time step due to the occurrence of nonlinear jump effects, which can occur when high bearing stiffness values are encountered. With excessive values of unbalance, damper lockup may occur.

In a later section, the Steady State Nonlinear Synchronous Unbalance responses will be evaluated for various values of rotor unbalance to illustrate damper lockup.

## Transient Motion at 150,000 RPM With Unbalance and Aerodynamic Excitation

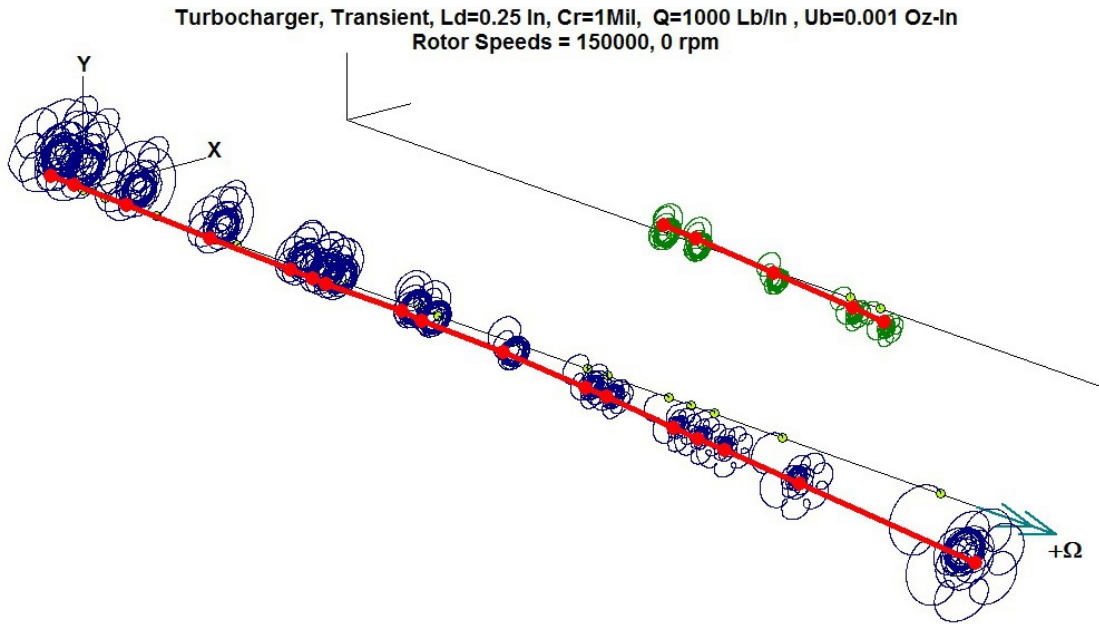


**Figure 4.4 Turbocharger Transient Motion at 150,000 RPM With Low  $U_b$  &  $Q$**   
 $L_d = 0.25$  In,  $C_d = 0.0001$ ,  $U_b = 0.001$  Oz-In,  $Q = 1000$  Lb/In

Figure 4.4 represents the time transient motion of the turbocharger with a low level of unbalance and an aerodynamic cross coupling of  $Q = 1,000$  lb/in. The system is marginally stable. The motion at the rotor center is synchronous.

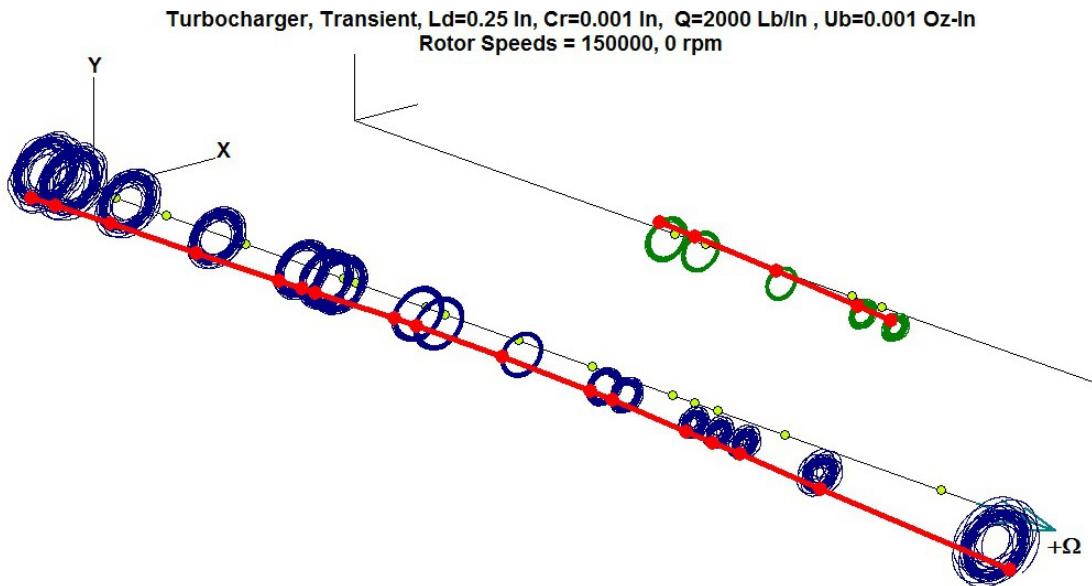


**Figure 4.5 Stable Turbocharger Motion With Aerodynamic  $Q = 2,000$  Lb/In**  
 $L_d = 0.25$  In,  $C_r = 0.001$  In,  $U_b = 0.001$  Oz-In

Figure 4.5 shows stable turbocharger motion from 20 to 50 cycles of motion with the aerodynamic cross coupling increased from 1,000 lb/in to 2,000 lb/in. With this low value of unbalance, the turbocharger remains in stable synchronous precession. After the initial 20 cycles of transient motion, which excites the first critical speed due to the suddenly applied gravity loading, the turbocharger remains stable.

# Turbocharger With Aerodynamic Q =1,000 Lb/In and High Unbalance Ub = 0.01 Oz-In

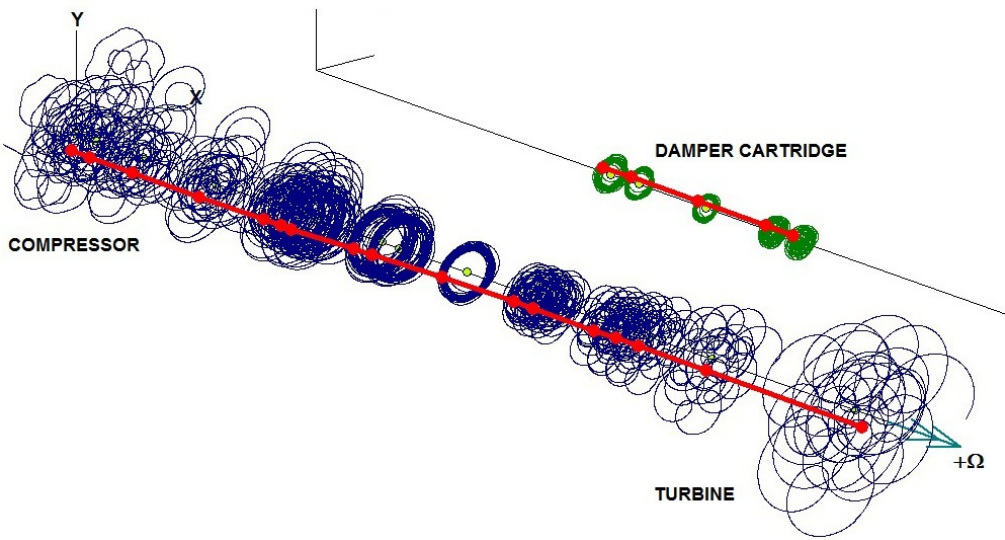


Fig. 4.6 Turbocharger Motion With Q =1,000 Lb/In and Ub= 0.01 Oz-In

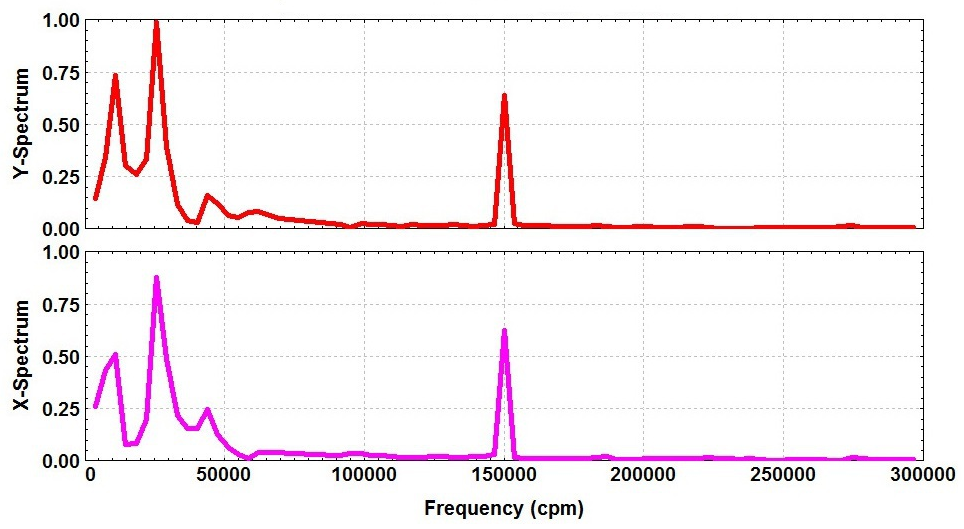


Figure 4.7 FFT With Q =1,000 Lb/In and Ub= 0.01 Oz-In

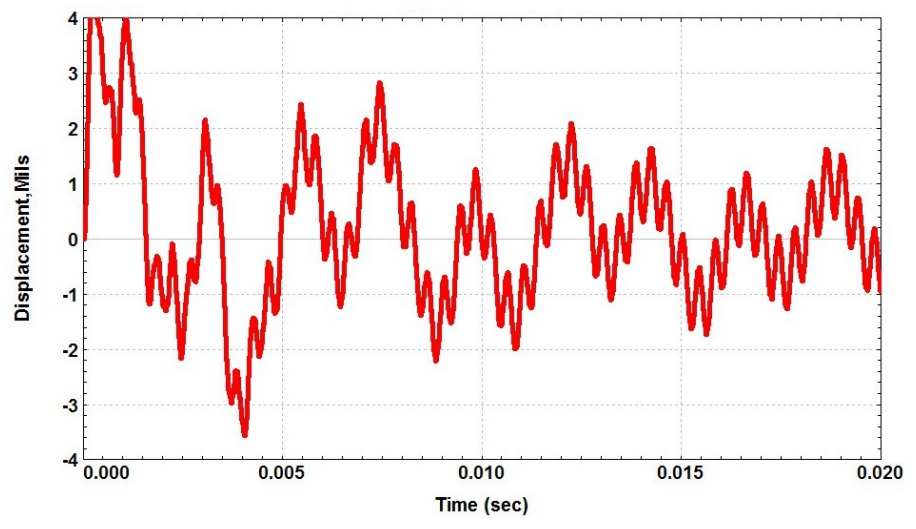


Fig. 4.8 Compressor Transient Motion With Q & Ub= 0.01 Oz-In

# Turbocharger Transient Motion Under Various Levels Of Aerodynamic Cross-Coupling, Q

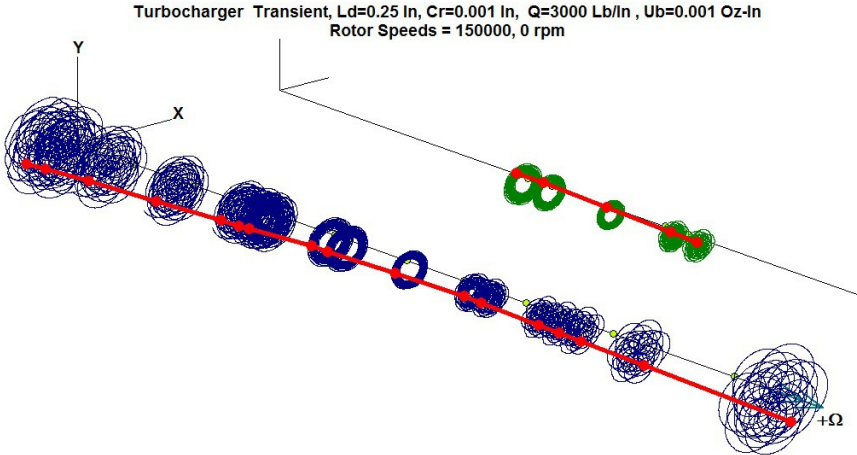


Fig. 4.9 Turbo Transient Motion With  $Q = 3000$  lb/in

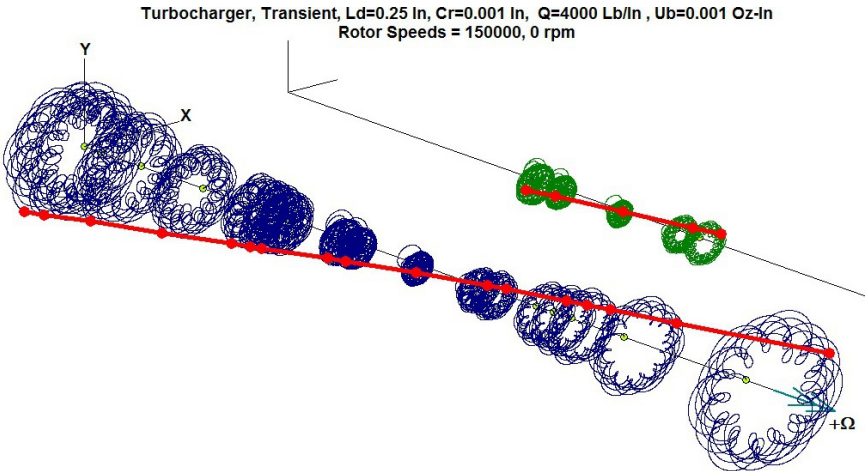


Fig. 4.10 Turbo Transient Motion With  $Q = 4000$  lb/in

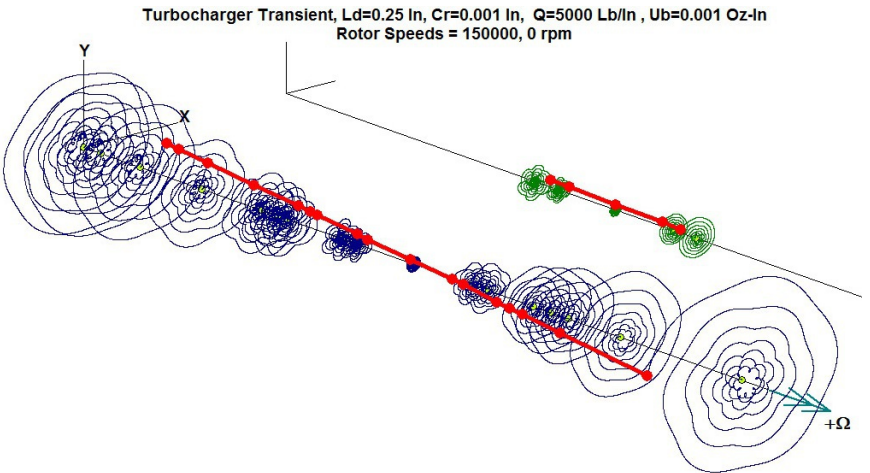


Fig. 4.11 Turbo Transient Motion With  $Q = 5000$  lb/in

## Summary of effects of Unbalance and Aerodynamic Excitation on Unstable Whirl Motion

Figure 4.4 and 4.5 shows that the turbocharger is stable with low unbalance and an aerodynamic excitation of  $Q = 1,000 \text{ lb/in}$ . In Figure 4.6, the aerodynamic excitation is a low value of  $Q = 1,000 \text{ lb/in}$ , however, the unbalance has been increased by an order of magnitude from  $0.001 \text{ Oz-in}$  to  $0.01 \text{ Oz-in}$ .

This significant increase in unbalance causes higher stiffness values to be generated in the squeeze film dampers. As a result of this, the whirl orbits are significantly increased. It is observed that both the first and second modes are excited in the initial transit response of the turbocharger. It will be demonstrated later that large increases in unbalance can result in damper lockup. When this occurs, it will be seen that the rotor will not be able to pass through the second critical speed.

Unlike a turbocharger in floating ring bearings, the source of whirl excitation for ball bearing turbochargers is the aerodynamic Alford forces generated on both the compressor and turbine impellers. Figure 4.9 shows the aerodynamic excitation  $Q$  increased to  $3,000 \text{ lb/in}$ . The motion is in limit cycle whirl motion and is still well contained. Figure 4.10 shows the aerodynamic excitation increased to  $4,000 \text{ lb/in}$ . In this case, limit cycle whirling is produced with the predominant mode of motion being the conical first speed mode of the turbocharger.

When the aerodynamic excitation is increased to  $Q = 5,000 \text{ lb/in}$ , the system is totally unstable and the whirl motion continues to spiral outward. At this level of aerodynamic excitation, the compressor impeller would contact the volute resulting in shaft failure. In this particular case, a higher level of aerodynamic excitation may be achieved by employing a centered damper design using O-rings.

## The Influence of Unbalance on Damper Lock Up With a Ball Bearing Turbocharger

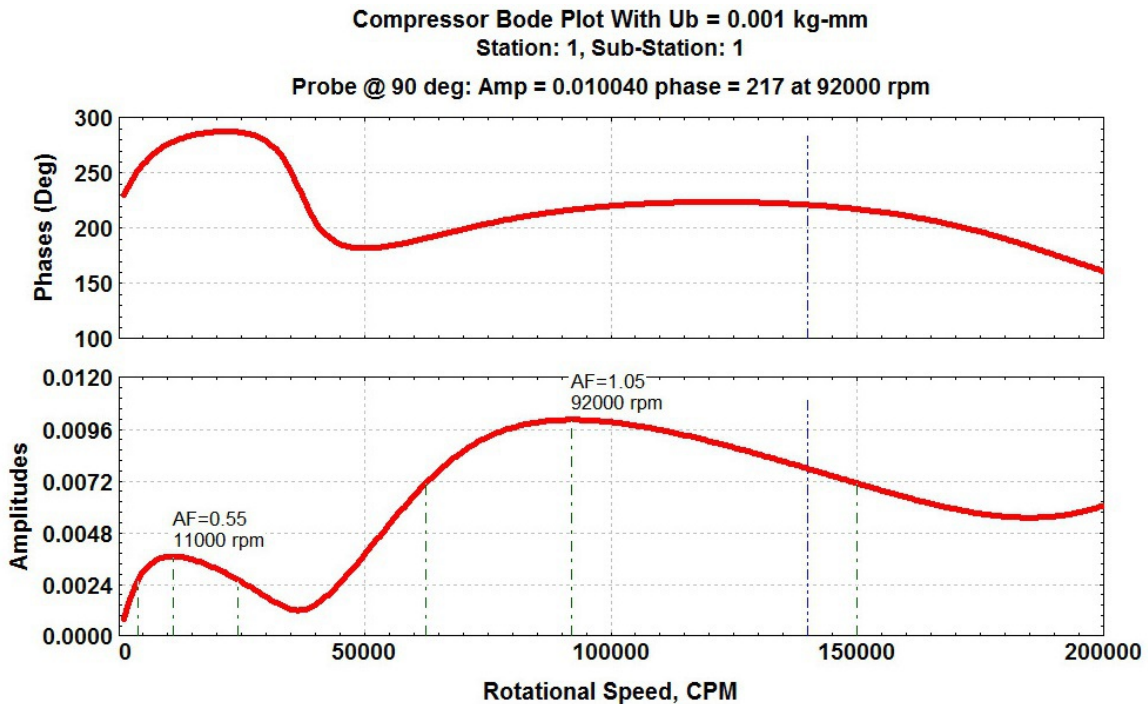


**Figure 4.12 Compressor Amplitude & Phase Response With Ub = 0.0014 Oz-In**

Figure 4.12 represents the compressor response with a low level of unbalance of  $0.0014 \text{ Oz-In}$  ( $0.001 \text{ kg-mm}$ ) placed at both the compressor and turbine wheels. The unbalance at the turbine is placed at a  $90^\circ$  angle to the compressor wheel unbalance so as to excite both the first and second turbocharger critical speeds. The first critical speed is excited at  $11,000 \text{ RPM}$  and the second critical speed is excited at  $92,000 \text{ RPM}$ . At the first critical speed, which is a conical mode, the amplitude at the turbine is the highest. At the second critical speed, the motion is largest at the compressor location.

# The Influence of Unbalance on Damper Lock Up With a Ball Bearing Turbocharger

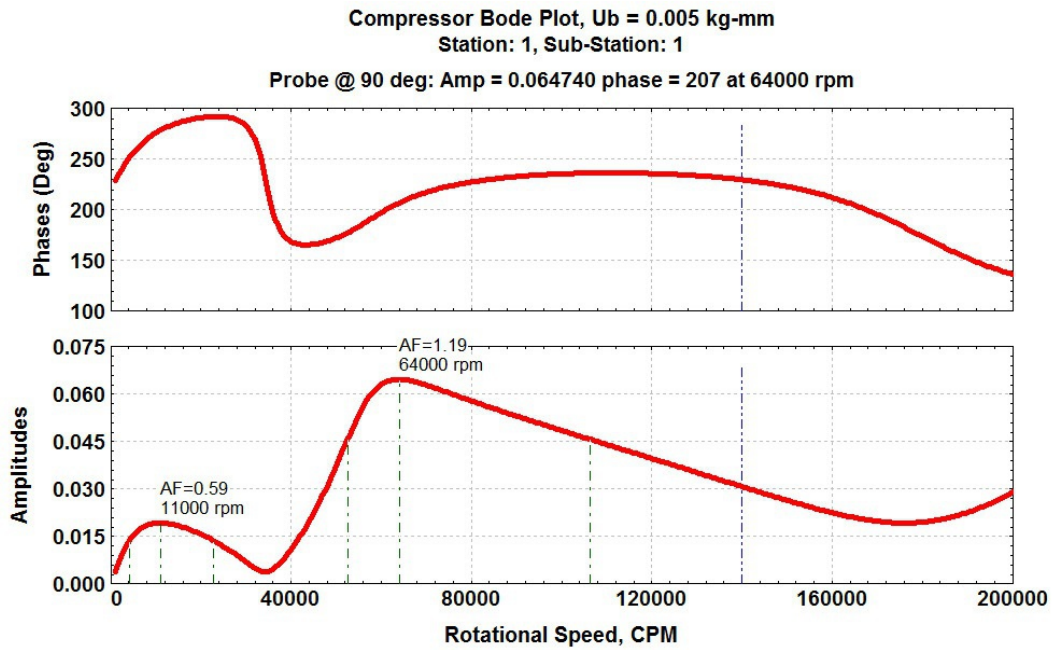


**Figure 4.13 Compressor Amplitude & Phase Response With  $U_b = 0.005$  kg-mm**

Figure 1.3 represents the compressor unbalance increased by a factor of fivefold from 0.001 kg-mm to 0.005 kg-mm. The new response generated shows some nonlinear behavior in the squeeze film dampers as the amplitude has increased from 0.010 in. to 0.0647 in. This represents a ratio of approximately 6.5 in the increase of amplitude with a 5 times increase in unbalance. There is also a significant change in the speed of maximum amplitude. With the lower lever of unbalance of 0.001 kg-mm, the maximum speed was computed to be at 92,000 RPM. With the unbalance increased to 0.005 kg-mm, there is a significant reduction in the computed speed of maximum amplitude to 64,000 RPM. This type of critical speed response does not change with a linear system.

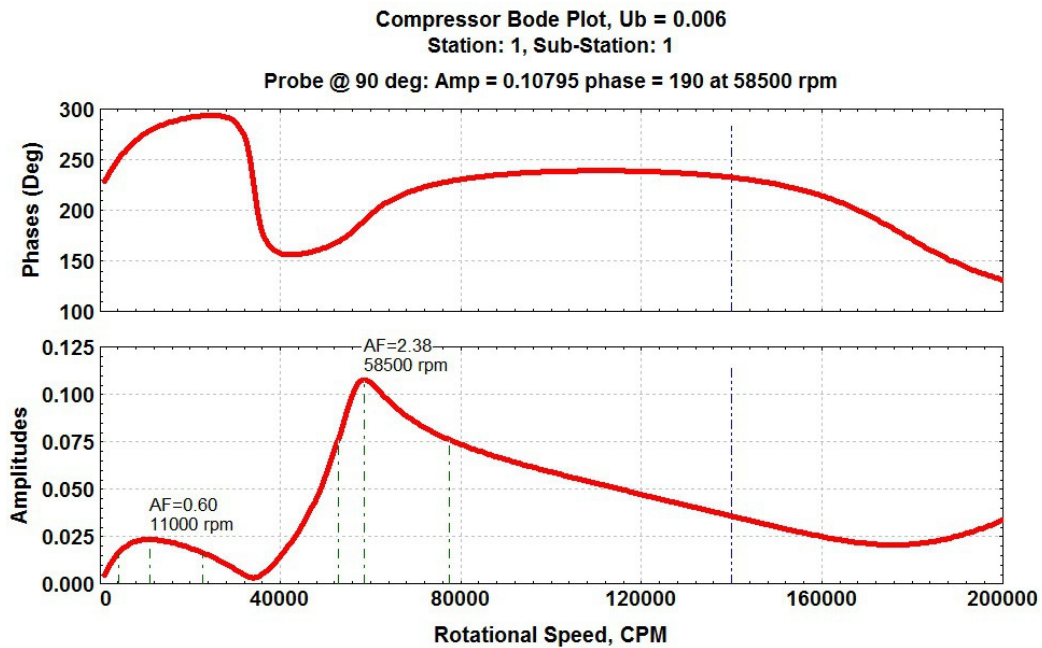


**Figure 4.14 Compressor Amplitude & Phase Response With  $U_b = 0.006$  kg-mm**

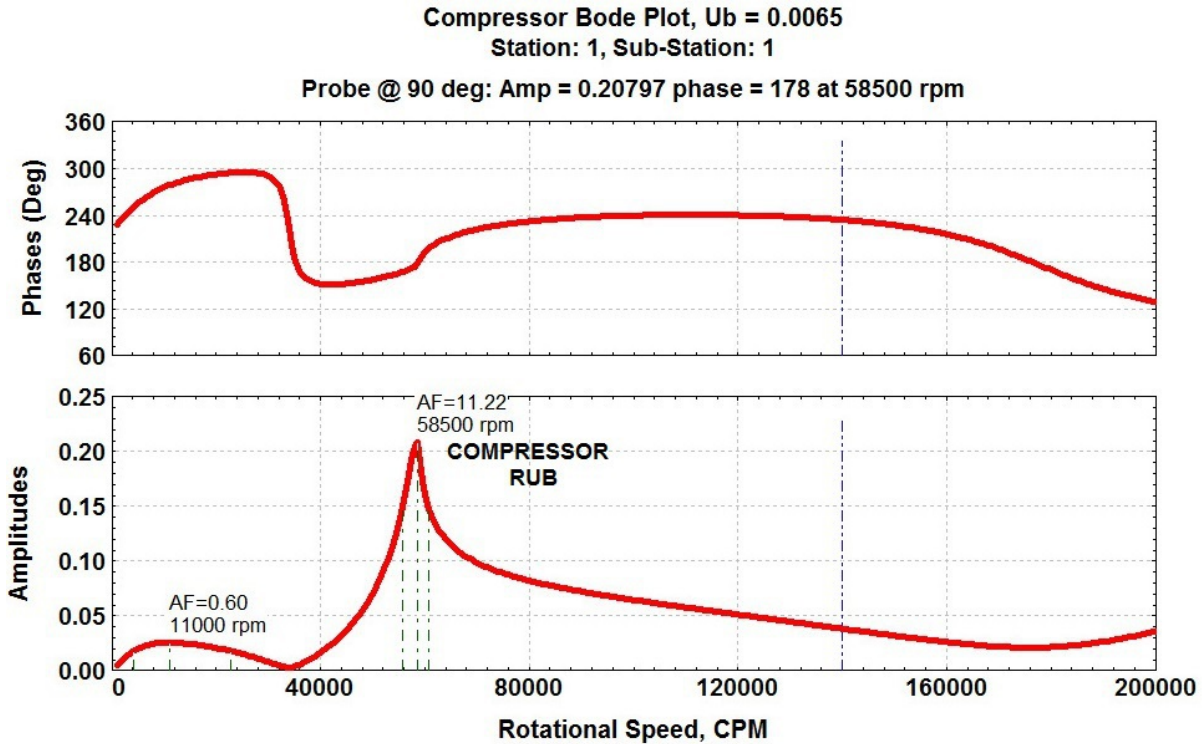


Figure 4.15 represents a dramatic increase in the doubling of the amplitude at 58,500 RPM of the compressor with only a small increase of the unbalance from 0.006 kg-mm to 0.0065 kg-mm. The response of the squeeze film damper at the compressor location has now entered into the highly nonlinear range. The large amplitudes encountered at the compressor location would now lead to the rubbing of the compressor impeller on the volute.

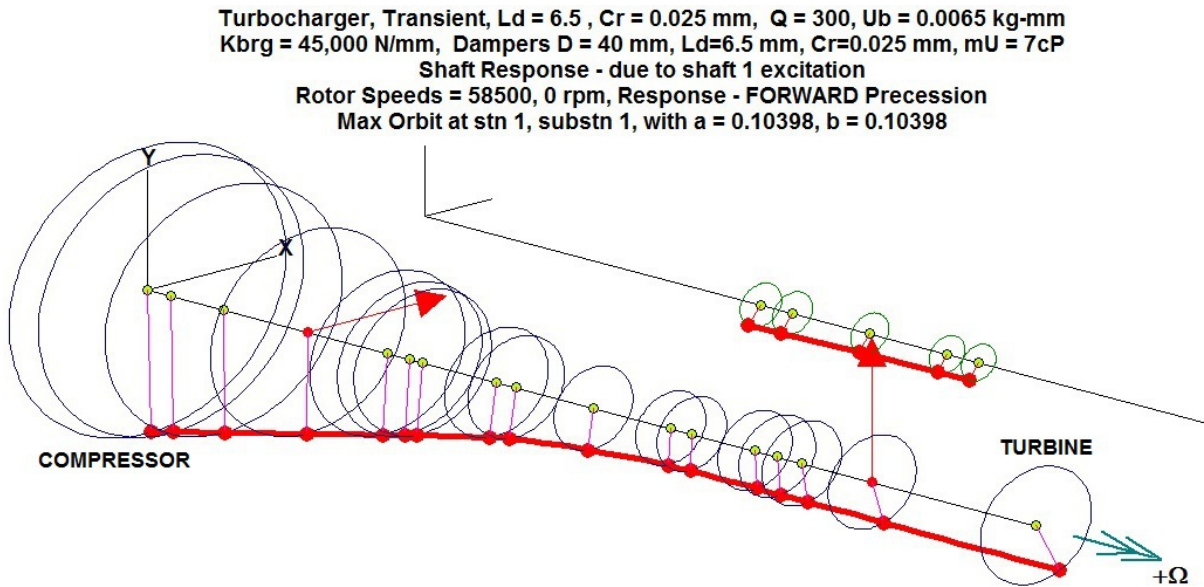


Figure 4.16 represents the turbocharger mode shape at the second critical speed at 58,500 RPM with the unbalance of 0.0065 kg-mm. It is the high vibrations that occur at the second critical speed that is responsible for bearing damage in both floating ring and ball bearing turbochargers.

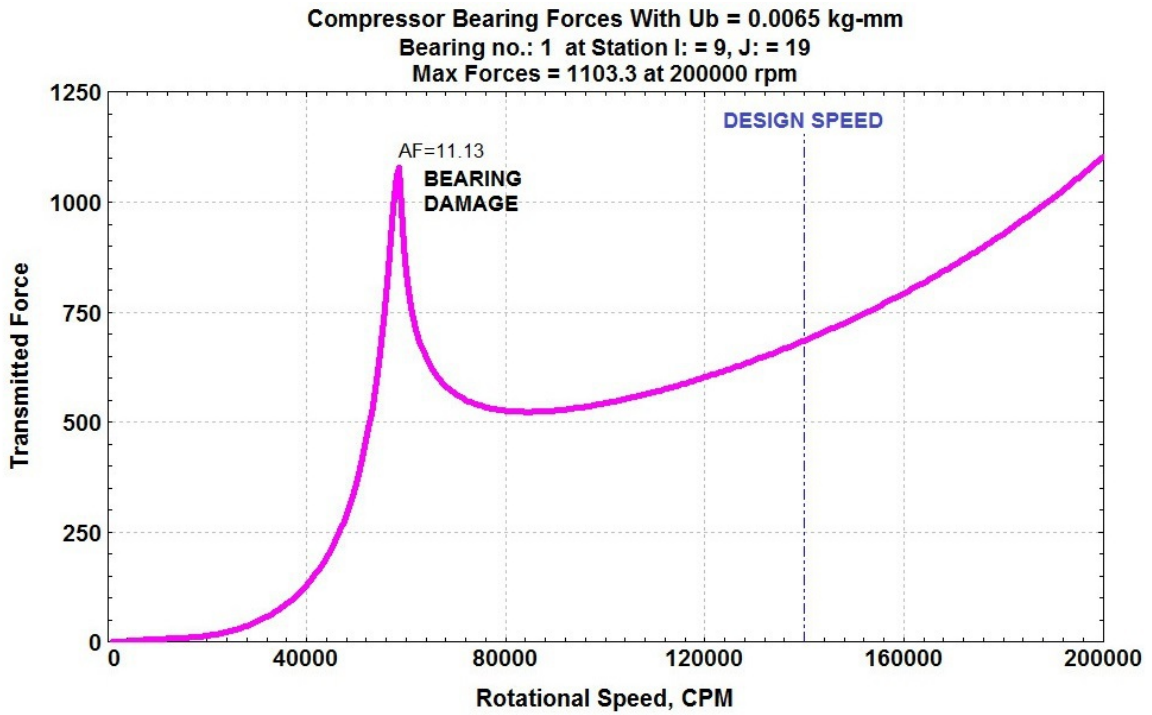


Figure 4.17 represents the transmitted compressor bearing forces with an unbalance of  $U_b = 0.0065$  kg-mm (0.009 Oz-in or 0.318 gm-in) placed at a  $90^\circ$  phase on the compressor and turbine impellers. It is the unbalance at the compressor location that has the greatest effect on the transmitted compressor bearing forces.

With all turbochargers, whether floating ring or rolling element design, the steel turbine impeller is heavier than the AL compressor. During operation through the second critical region, the compressor and turbine impeller motions are now in phase. Since the turbine is heavier than the compressor, the turbine amplitudes and bearing forces, when operating through this region are always lower than the amplitudes and bearing forces encountered at the compressor and the compressor bearing. It has been observed with all failed turbochargers, regardless of bearing type, there is always significant damage to the compressor bearing

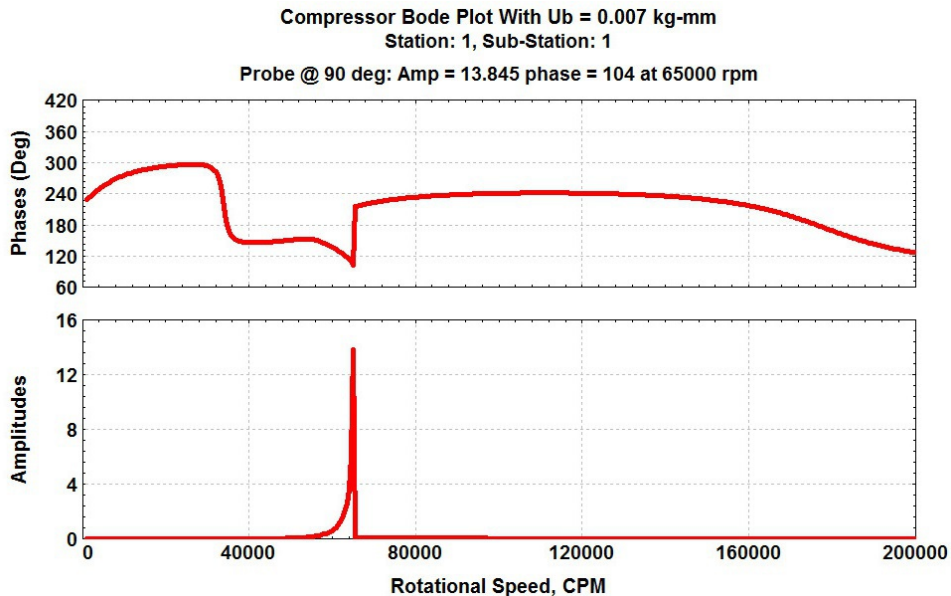
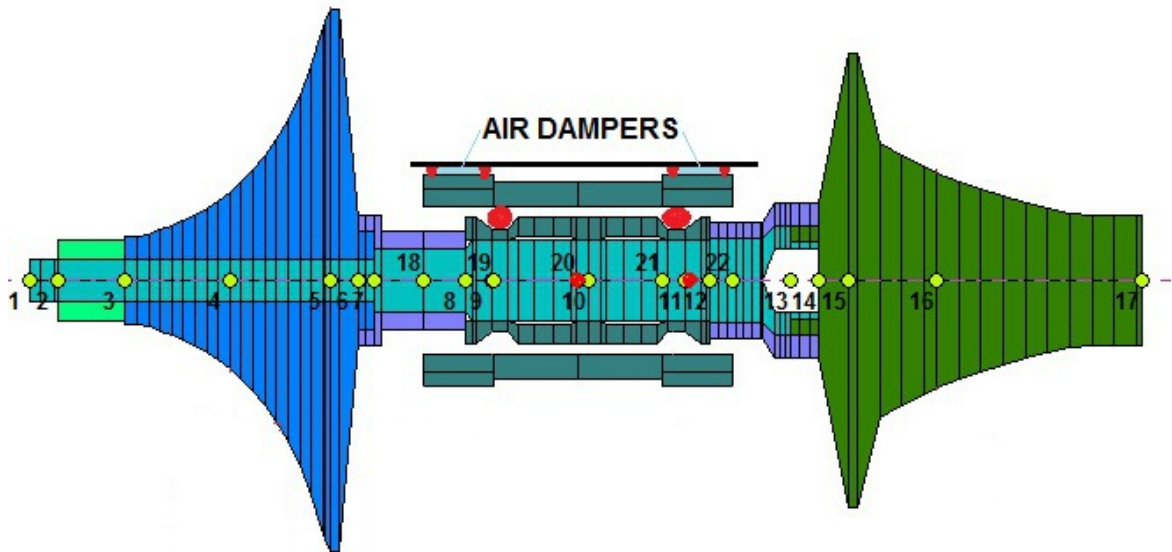


Figure 4.18 shows failure of the turbocharger with the unbalance increased to 0.007 kg-mm.

## 5 Dynamic Analysis of a Ball Bearing Turbocharger in Air Squeeze Film Dampers



**Figure 5.1 Ball Bearing Turbocharger in an Air Squeeze Film Damper**

Figure 5.1 represents a ball bearing turbocharger with two closed end air squeeze film dampers installed. The air squeeze dampers are enclosed by two close-fitting O-rings to form a sealed air damper chamber. The air damper volume is sealed and does not require a supporting pressurized air supply, as the dampers are self contained.

The concept of air squeeze film dampers is not new. This concept has been utilized in high-speed dental drills since 1965. As previously mentioned in Section 1, a squeeze film damper system has been successfully installed in an aircraft ball bearing ACM unit operating at 100,000 RPM.

The stiffness of the damper system is basically determined by the O-ring material and the design of the closely fitting O-ring grooves in the damper cartridge. The effective stiffness of the rubber O ring support system generally has to be determined by a load-deflection test with the O-rings installed in the close-fitting grooves.

When the rubber O rings are under load situated in tight fitting grooves, they will exhibit some nonlinear stiffness effects, which is beneficial for providing for limit cycle whirling under conditions of large Alford instability forces generated by both the compressor and turbine impellers. The exact magnitude of these forces are difficult to compute in advance and require experimental testing.

Table 5.1 represents the stiffness and damping characteristics of various squeeze film damper configurations with open and closed end dampers. The damping characteristics have been computed for either a  $\pi$  or  $2\pi$  film extent. The characteristics of the an uncentered oil film damper, for example, are based on an open ended cavitated  $\pi$  film. As such, oil film dampers, in addition to generating damping, have highly nonlinear stiffness characteristics which increase rapidly with eccentricities exceeding 0.5.

This is in stark contrast to the characteristics of an enclosed air film damper, which is based on a  $2\pi$  uncavitated fluid film which will develop damping but no stiffness. Hence, by not having a highly nonlinear stiffness generated by the damper, the condition of damper lockup is avoided. This characteristic represents a significant improvement over what is encountered with uncentered oil squeeze film dampers.

Bearing	Film	Motion	Stiffness	Damping
Short Bearing	$\pi$ film	Circular Synchronous Precession	$\frac{2\mu R L^3 \varepsilon \omega}{C^3(1-\varepsilon^2)^2}$	$\frac{\mu R L^3 \pi}{2C^3(1-\varepsilon^2)^{3/2}}$
	$2\pi$ film		0	$\frac{\mu R L^3 \pi}{C^3(1-\varepsilon^2)^{3/2}}$
	$\pi$ film	Pure Radial Squeeze Motion	0	$\frac{\mu R L^3 \pi (2\varepsilon^2 + 1)}{2C^3(1-\varepsilon^2)^{5/2}}$
	$2\pi$ film		0	$\frac{\mu R L^3 \pi (2\varepsilon^2 + 1)}{C^3(1-\varepsilon^2)^{5/2}}$
Long Bearing	$\pi$ film	Circular Synchronous Precession	$\frac{24\mu R^3 L \varepsilon \omega}{C^3(2+\varepsilon^2)(1-\varepsilon^2)}$	$\frac{12\mu R^3 L \pi}{C^3(2+\varepsilon^2)(1-\varepsilon^2)^{1/2}}$
	$2\pi$ film		0	$\frac{24\mu R^3 L \pi}{C^3(2+\varepsilon^2)(1-\varepsilon^2)^{1/2}}$

Where

$R$  = damper radius

$L$  = damper axial length

$C$  = radial clearance

$\omega$  = whirl speed

$\mu$  = oil viscosity

$\varepsilon$  = eccentricity ratio

**Table 5.1 Stiffness and Damping Characteristics of Cavitated and Uncavitated Squeeze Film Dampers Under Open and Closed End Conditions**

## Air Squeeze Film Damping Characteristics For Various Lengths and Radial Clearances

Ecc	C=0.001 L = 0.5	C=0.00125 L = 0.5	<b>C=0.0015</b> <b>L = 0.5</b>	C=0.00175 L = 0.5	C=0.0015 L = 0.6	C=0.002 L = 0.6
0.0	23.1	11.8	<b>6.8</b>	4.3	8.2	3.5
0.3	23.1	11.8	<b>6.85</b>	4.3	8.2	3.5
0.5	23.6	12.1	<b>7.0</b>	4.4	8.4	3.55
0.7	25.9	13.3	<b>7.7</b>	4.8	9.2	3.9
0.8	29.0	14.9	<b>8.6</b>	5.4	10.5	4.4
0.9	37.7	19.3	<b>11.2</b>	7.0	13.4	5.6
0.95	50.9	26.0	<b>15.0</b>	9.5	18.1	7.6

**Table 5.2 Closed End Air Damping Coefficients For Various Damper Lengths and Clearances**  
**D = 1.5 In,  $\mu = 2.9e-9$  Reyns**

Table 5.2 shows the damping generated with a closed end air squeeze film damper for various damper lengths and clearances. What is highly desirable about the air squeeze film damper is that it does not generate a radial stiffness similar to that of an oil squeeze film damper. As such damper lockup will not occur with an air squeeze film damper caused by excessive stiffness generated in the squeeze film damper due to unbalance.

The stiffness of an air squeeze film damper is primarily due to the material properties of the rubber O-rings, O-ring preload and the design of the close fitting O-ring grooves.

In Table 3.1, on the turbocharger stability for various values of support damping and stiffness, it was seen that from aerodynamic cross coupling Q of = 1000 lb/in, that a damping between 5 and 10 lb-s/in would be satisfactory. Therefore, from the above Table 5.2 is seen that a squeeze film damper with a length of 0.5 inches and the radial clearance of 0.0015 inches would be satisfactory.

$$C_d = \frac{24\mu R^3 L\pi}{C^3(2 + \varepsilon^2)(1 - \varepsilon^2)^{1/2}} \quad 5.1$$

Equation 5.1 represents the damping generated by the closed end air squeeze film damper. Note that the damping is highly linear up to an eccentricity of 0.7. After the eccentricity exceeds 0.8, the damping it becomes highly nonlinear. This is actually not a disadvantage as it helps control limit cycle whirling.

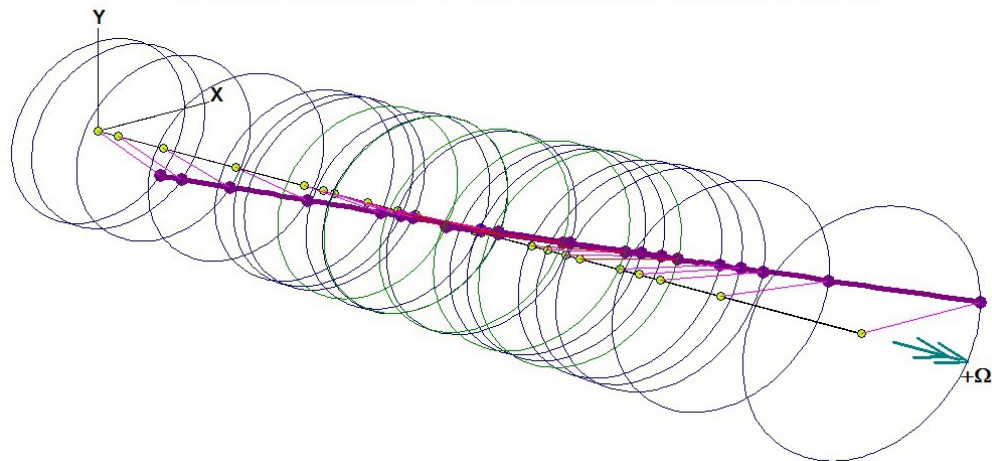
The oil squeeze film damper had a length of 0.25 in and a clearance of 0.001 in. This clearance is considered to be on the tight side. With the air damper with an assumed length of 0.5 and a clearance of 0.001 in, the predicted damping is 23 lb-s/in. Opening up the clearance to 0.0015 in provides adequate damping for stability control. The damping generated with the longer length damper of 0.6 in and the larger clearance of 0.002 in would produce damping of only 3 to 4 lb-s/in which would be inadequate.

## Turbochargers Stability in Air Squeeze Film Dampers

The stability of the turbocharger with respect to aerodynamic cross coupling acting on the compressor and turbine wheels will be computed assuming an air squeeze film damper with the equivalent stiffness of 5,000 lb/in and an effective damping of 7.0 lb-s/in. This will be equivalent to assuming a squeeze damper with a length of 0.5 in and a radial clearance of 0.0015 in.

The assumed value of the damping of 7 lb-s/in may be considered as conservative as there will be some contribution from the damping provided by the O-rings. The air viscosity of  $2.9E-9$  Reysn was assumed for a temperature of  $140^{\circ}$  F. The operating temperature of the turbocharger at the dampers will be considerably higher than this value. For air, as the temperature increases, there is also a corresponding increase in viscosity.

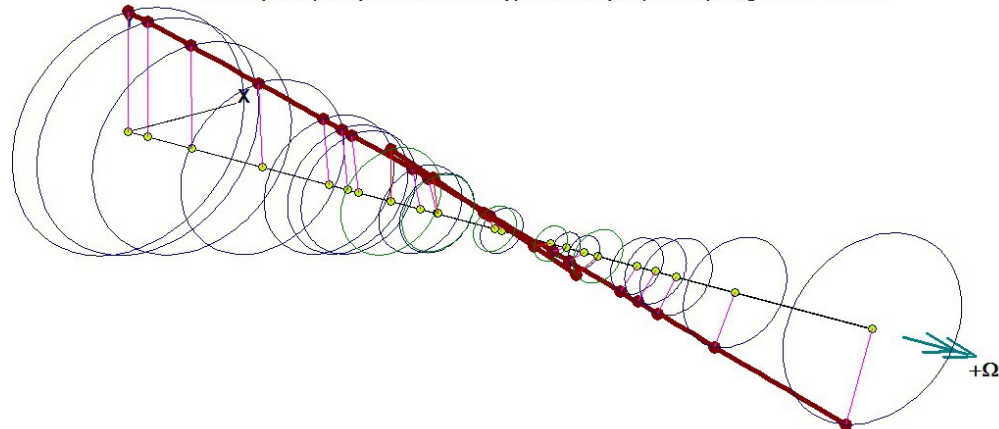
Turbocharger Air Dampers,  $K_d = 5000$  Lb/In,  $L_d = 0.50$ ,  $C_r = 0.0015$ ,  $C_d = 7$  Lb-S/In,  $Q = 1000$  Lb/In ,  
 $K_{brg} = 250,000$  Lb/In,  $D = 1.5$ ,  $N = 150,000$  RPM  
 Mode No.= 3 STABLE : Rotor: 1 FORWARD : Rotor: 2 FORWARD Precession  
 Shaft Rotational Speeds = 150000, 0 rpm  
 Whirl Speed (Damped Natural Freq.) = 7598 rpm (127 Hz), Log. Dec. = 5.0290



### 5.2 1<sup>st</sup> Forward Turbocharger Whirl Mode at 7598 CPM, $L_d = 5$

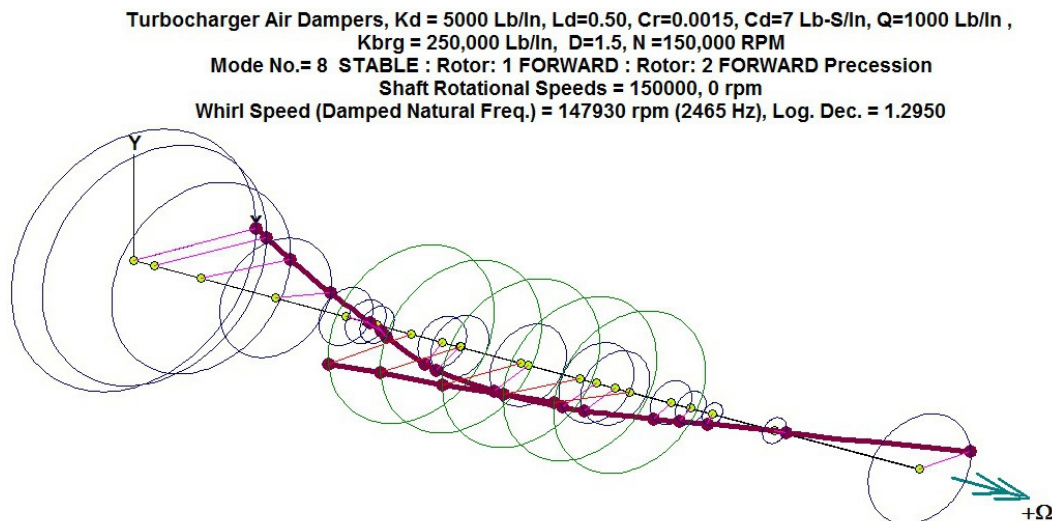
Figure 5.2 represents the first turbocharger forward whirl mode at 7598 CPM computed with an aerodynamic cross coupling of  $Q = 1,000$  lb/in at 150,000 RPM. This mode is highly stable and since the log decrement is greater than 3.14, this mode will not be excited by unbalance.

Turbocharger Air Dampers,  $K_d = 5000$  Lb/In,  $L_d = 0.50$ ,  $C_r = 0.0015$ ,  $C_d = 7$  Lb-S/In,  $Q = 1000$  Lb/In ,  
 $K_{brg} = 250,000$  Lb/In,  $D = 1.5$ ,  $N = 150,000$  RPM  
 Mode No.= 4 STABLE : Rotor: 1 FORWARD : Rotor: 2 FORWARD Precession  
 Shaft Rotational Speeds = 150000, 0 rpm  
 Whirl Speed (Damped Natural Freq.) = 20363 rpm (339 Hz), Log. Dec. = 1.7097



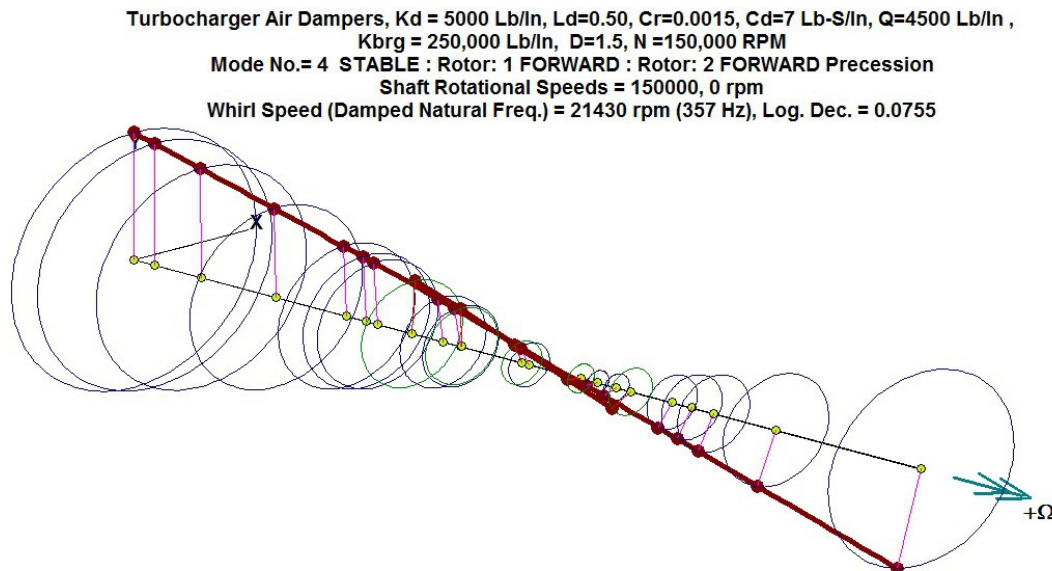
### 5.3 2<sup>nd</sup> Forward Turbocharger Whirl Mode at 20,363 CPM, $L_d = 1.7$

Figure 5.3 represents the second forward whirl mode computed at 20,363 CPM. This is a conical whirl mode and as can be seen with the log decrement of 1.7, the system is highly stable. It will be seen in that the air squeeze film dampers will be able to sustain an aerodynamic cross coupling Q value of over 4,000 lb/in.



#### 5.4 3rd Forward Turbocharger Whirl Mode at 147,930 CPM, $L_d = 1.3$

Figure 5.4 represents the third turbocharger whirl mode computed at 147,930 CPM. This mode could be of concern because it corresponds to the running operating speed of 150,000 RPM. Although this third critical speed corresponds to running speed, it will be seen that it is well damped and should not be a problem.



#### 5.5 2<sup>nd</sup> Forward Turbocharger Whirl Mode at 21,430 CPM, $L_d = 0.076$ Aero Cross Coupling $Q = 4,500 \text{ Lb/In}$

Figure 5.5 represents the turbocharger conical whirl mode with an aerodynamic cross coupling of  $Q = 4,500 \text{ lb/in}$ . It is seen that the turbocharger is on the threshold of stability. The air squeeze film damper has a significant ability to resist self excited aerodynamic whirl instability. It is seen that a properly designed centered air squeeze film damper may be superior to an uncentered oil damper.

## Turbocharger Unbalance Response in Air Squeeze Film Dampers

In this section, the unbalance response of a turbocharger mounted in air squeeze film dampers will be computed to review the synchronous response and bearing forces transmitted over the operating speed range. Figure 5.6 represents the nonlinear unbalance response of the turbocharger compressor and turbine impellers over a speed range up to 200,000 RPM.

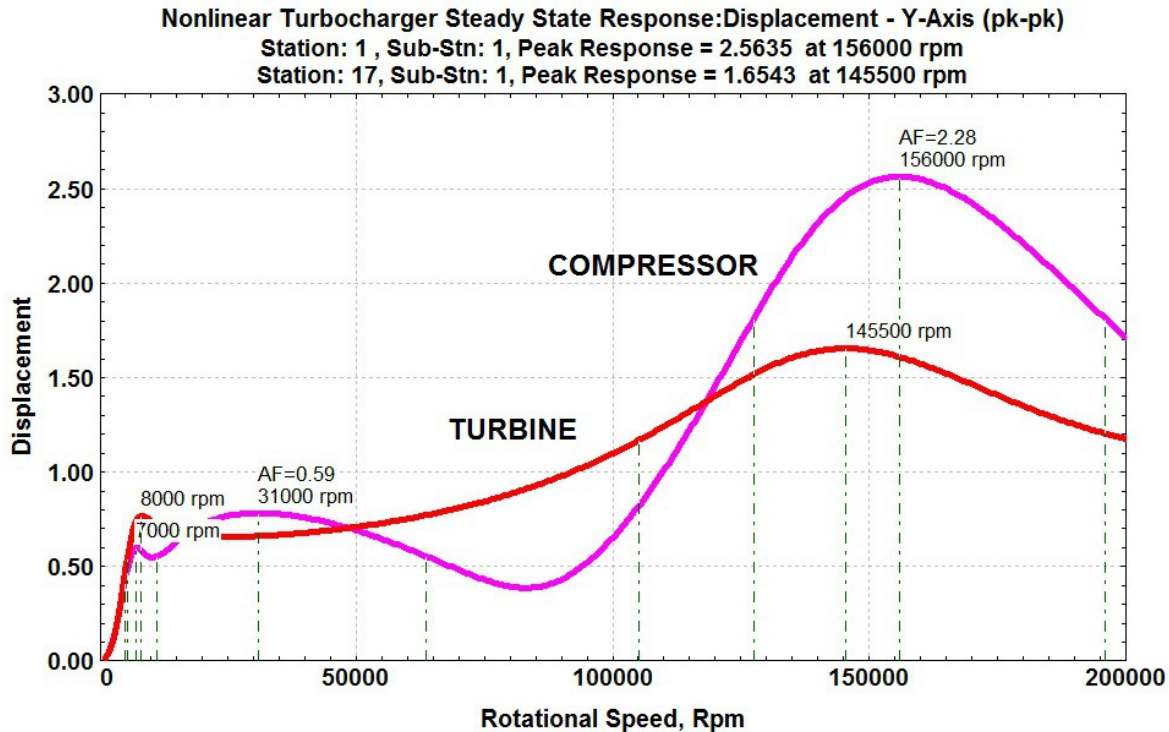


Figure 5.6 Turbocharger Nonlinear Unbalance Response in Air Squeeze Film Dampers

Figure 5.6 represents the nonlinear synchronous unbalance response of the turbocharger over a speed range to 200,000 RPM. The nonlinear response shows that the peak amplitude for the compressor impeller occurs at a speed of 156,000 RPM with an amplification factor of 2.28. The peak amplitude at the turbine occurs at 145,500 RPM.

The maximum amplitudes at the impellers are 2.6 Mills P-P at the compressor and only 1.65 Mills at the turbine. In this particular design of turbocharger, the third bending critical speed is occurring near the design operating speed of 150,000 RPM. The occurrence of the turbocharger 3<sup>rd</sup> bending critical speed in the operating speed range is not a serious problem as the amplification factors for the compressor and turbine impellers are small. This third bending critical speed of the turbocharger may be elevated by increasing the shaft diameter.

Also of important to note from Table 5.2 is that the damping coefficients for the air squeeze film damper are highly linear up to an eccentricity of 0.7. At an eccentricity of 0.9 and above, the damping doubles in value. As previously noted, the characteristics of nonlinearity in the air squeeze film damper are not an undesirable feature as compared to the nonlinear stiffness behavior of the oil squeeze film damper, which is highly undesirable.

It will be shown that the dynamic response analysis of an air squeeze film damper may be taken as a linear system with high accuracy. Figure 5.7 represents the dynamic unbalance response of the turbocharger, assuming a linear squeeze film damper system with a stiffness of  $K_d = 5,000$  lb/in and damping of  $C_d = 7$  lb/s/in.

## Turbocharger Unbalance Response in Air Squeeze Film Dampers

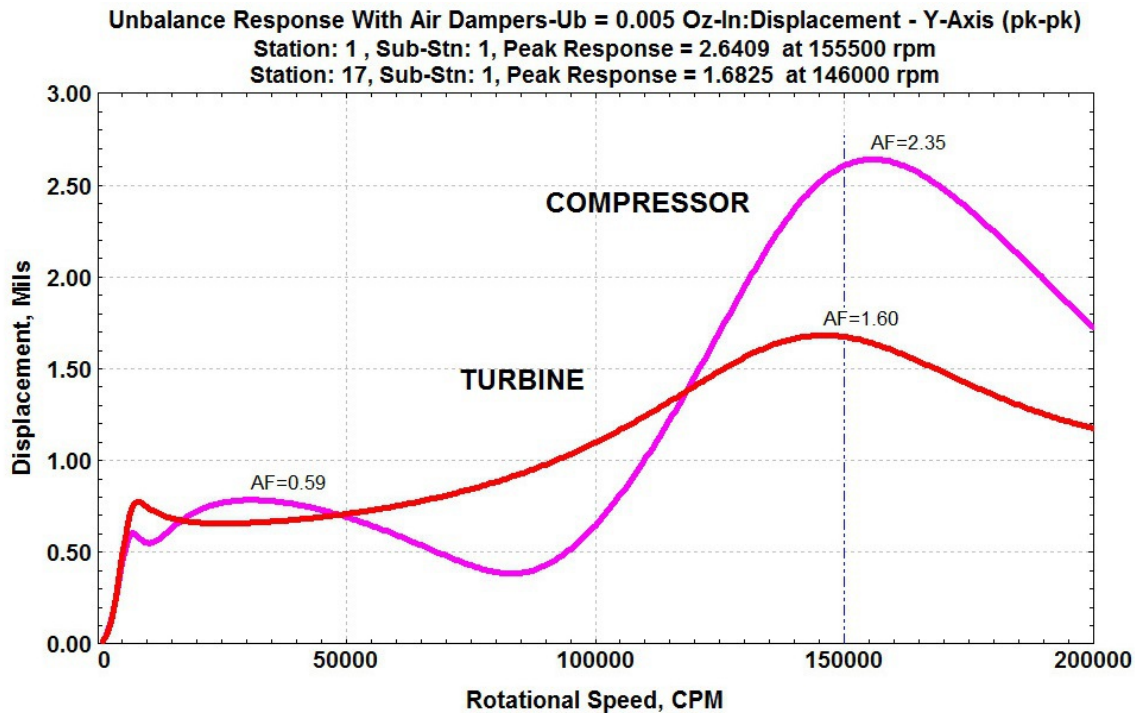


**Figure 5.7 Turbocharger Linear Unbalance Response in Air Squeeze Film Dampers**

Figure 5.7 represents the linear unbalance response of the turbocharger in the air squeeze film dampers. The comparison between the maximum amplitudes at the compressor and turbine locations between the nonlinear and linear models are very close. For example with the nonlinear analysis, the maximum compressor amplitude is 2.56 Mils at 156,000 RPM. The maximum amplitude for the compressor based on linear analysis is 2.64 Mils at 155,500 RPM. One may conclude when analyzing the dynamics of turbochargers in air squeeze dampers that linear analysis may be used with high accuracy.

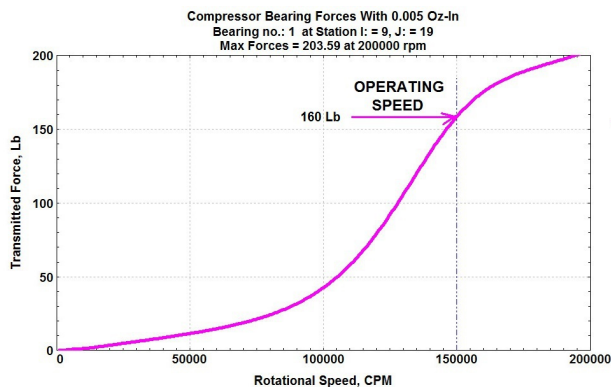


**Figure 5.8 Compressor Bearing Forces**

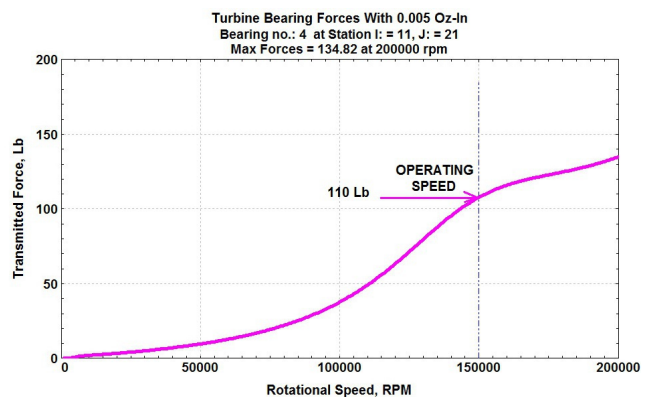


**Figure 5.9 Turbine Bearing Forces**

Figures 5.8 and 5.9 represent the forces transmitted to the compressor and impeller rolling element bearings at the design speed of 150,000 RPM. Note that the loads transmitted to the compressor bearing are 160 lb as compared to the lower forces transmitted to the turbine bearing of 110 lb.

Once the turbocharger passes through the second critical speed region, due to the higher mass of the turbine impeller, the rotor mode shape is always larger at the compressor location. As a result, all failed turbochargers, whether rolling element or floating bush film bearings, show extensive damage at the compressor bearing location.

## Turbocharger Unbalance Response in Air Squeeze Film Dampers

Turbocharger Air Dampers,  $K_d = 5000 \text{ Lb/in}$ ,  $L_d = 0.50$ ,  $C_r = 0.0015$ ,  $U_b = 0.005$   
 $K_{brg} = 250,000 \text{ Lb/in}$ ,  $D = 1.5$ ,  $N = 150,000 \text{ RPM}$   
Shaft Response - due to shaft 1 excitation  
Rotor Speeds = 150000, 0 rpm, Response - FORWARD Precession  
Max Orbit at stn 1, substn 1, with  $a = 0.0012652$ ,  $b = 0.0012652$

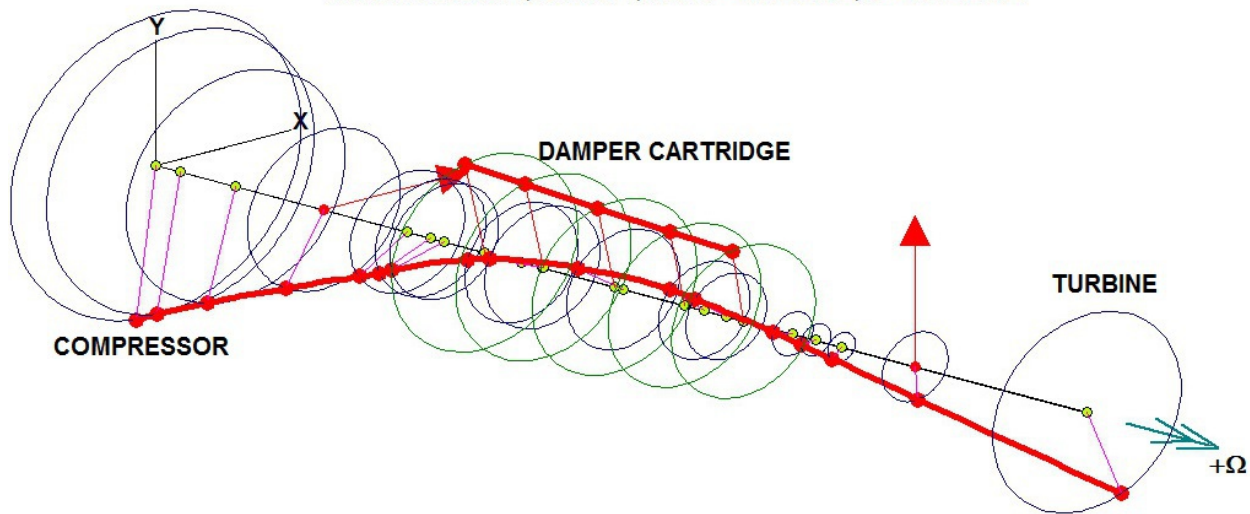


Figure 5.10 Turbocharger Mode Shape at 150,000 RPM

Figure 5.10 represents the mode shape of the turbocharger at 150,000 RPM with unbalance situated at both the compressor and turbine impellers. It should be noted that if the unbalance were situated only at the turbine impeller, the amplitude at the compressor would still be larger than the turbine response.

The high response of the compressor at the design speed should always be of some concern. If the compressor impeller should contact the volute, rubbing would occur that could cause the compressor wheel to go into a violent backward whirl mode. This violent backward whirling of the compressor would then cause a torsional failure of the shaft at the junction to the turbine impeller.

As can be seen from Figure 5.7, the design speed is near the third turbocharger bending critical speed. With the current design of the air squeeze film damper, this is not a serious problem. However if the amplitude at the design speed at the compressor needs to be reduced, this can be accomplished by increasing the diameter of the shaft to elevate the third bending critical speed.

### Discussion and Conclusions of Turbocharger Response in Air Squeeze Film Dampers

The use of closed end air squeeze film dampers appear to have significant advantages over the use of uncentered oil squeeze film dampers. The reason is that in addition to the fact that no fluid is required to supply the damper, air squeeze film dampers generate no radial stiffness forces and the damping forces are very linear over a large range of eccentricities.

The stiffness characteristics of a typical air squeeze film damper are determined by the O-ring material properties and the design of the tight fitting O-rings grooves. Since air squeeze film dampers do not develop the highly nonlinear radial stiffness forces encountered with oil squeeze film dampers, damper lockup due to moderate or high levels of unbalance, does not occur with air squeeze film dampers. This represents a huge advantage over typical oil squeeze film dampers, whether uncentered or centered.

The use of air squeeze film dampers is not new. They have been employed since 1965 for use in high speed dental drills. In summary, a well designed air squeeze film damper system should provide superior dynamic characteristics and improved bearing life as compared to the uncentered oil squeeze film dampers being used with the current design of turbochargers presently on the market.

## 6 Discussion and Conclusions

The dynamic characteristics of a ball bearing turbocharger mounted in an uncentered oil squeeze film damper are compared to the dynamical behavior of a ball bearing turbocharger supplied with a closed end air squeeze film damper system.

The standard type of turbocharger bearing that has been used for most conventional automotive and diesel engine turbochargers has been the floating bush bearing. The floating bush bearing has the advantage that it is inexpensive to produce. The use of floating bush bearings for turbochargers in large diesel engine have been very successful.

The reason for the success and the predominance of floating bush bearings in these large diesel engines is that, for one, the turbochargers operate at lower speeds as compared to automotive turbochargers, and second, with commercial diesel engines, the engines are kept idling as much as possible when parked.

This procedure enables the floating bush bearings to be well lubricated, and the slower operating speeds of the turbochargers results in controlled subsynchronous limit cycle whirl motion. Limit cycle whirling is always present in all floating bush bearing turbochargers.

The primary problem with automotive high-speed turbochargers is that floating bush bearings are inherently unstable. That is, the turbochargers are in a constant state of self-excited subsynchronous whirl motion, exciting either the first or second critical speeds of the turbocharger. A typical failure occurs when the turbocharger compressor impeller contacts the volute due to compressor bearing wear. This causes the impeller to precess in a backward motion resulting in shaft failure. Another problem with floating bush bearings is the inherent torsional drag of the floating bush bearing, which limits the rate at which the turbocharger may accelerate, which is referred to as turbo lag.

A more advanced and expensive generation of turbochargers have been developed using rolling element bearings, particularly with ceramic bearings. These turbochargers can operate to speeds exceeding 150,000 RPM. The problem with all ball bearing turbochargers is that the bearings are highly susceptible to bearing loads. For example, the bearing life of a rolling element bearing varies inversely as the cube of the bearing loads. Hence, a doubling of the bearing load causes the bearing life to be reduced by a factor of eight!

Ball bearing turbochargers do not suffer the type of inherent self-excited bearing instability that occurs with floating bush bearings. However, turbocharger instability can still occur at high power levels due to the presence of the cross coupling Alford forces generated on both the turbine and compressor impellers. These unstable Alford forces can excite both the turbocharger first and second rotor critical speeds

In order to protect ball bearing turbochargers from self-excited whirl instability and the lack of damping when passing through the critical speeds, oil squeeze film dampers are employed. Oil squeeze film dampers, for example, are universally used in all aircraft engines. However, with aircraft engines, a centering spring is employed due to the weight of the engine.

With the current design of ball bearing turbochargers, an uncentered oil squeeze film damper is employed. These squeeze film dampers usually have very narrow lands and tight damper clearances to provide damping for stability and critical speed control.

However, the use of uncentered dampers presents a problem in that it is virtually impossible to properly design a desirable combination of both stiffness and damping for the oil squeeze film dampers. One of the major problems with all oil squeeze film dampers is that the bearing radial stiffness increases rapidly with damper eccentricities exceeding .5. Thus, with moderate to large values of unbalance, the increase in stiffness, while passing through the second critical speed region can prevent unbalance phase inversion from occurring. Without proper phase inversion of the rotor mass center to occur, the amplitude, particularly at the compressor impeller continues to increase until contact with the volute occurs. This situation is referred to as damper lockup.

If a significant rub of the compressor impeller occurs on the volute, then the compressor wheel will proceed into a violent backward whirl motion, causing a torsional failure at the junction to the shaft to the turbine hub.

Improvements in uncentered oil squeeze film dampers could be achieved by using centered damper cartridges with O-rings. Currently this design configuration has not been utilized in any commercial ball bearing turbochargers .

In this paper, the dynamic characteristics of centered air squeeze film dampers are evaluated. As previously mentioned, the concept of an air squeeze film damper is by no means unique, as air squeeze film dampers have been employed in high-speed dental drills since the early nineteen sixties. The use of the air squeeze damper provides some unique features in that the damping is very linear over a high range of eccentricities. The basic stiffness of an air squeeze damper is provided by the rubber O-rings. As such, damper lockup does not occur with air squeeze film dampers.

The author has demonstrated that the use of a closed end air squeeze film damper is practical, as one has been successfully installed on an aircraft ACM unit operating at 100,000 RPM. The obvious advantage of an air squeeze film damper is that no external fluid is required to be supplied to the damper. Since the air squeeze film damper remains essentially linear up to an eccentricity approaching 0.8, the design analysis may be performed accurately using linear theory.

Although the amount of damping is small from an air squeeze film damper, for the typical high speed ball bearing turbocharger as illustrated, it has been demonstrated that the centered closed end air squeeze film air damper design is superior to an uncentered oil squeeze film damper with narrow lands and tight clearances. The centered closed end air damper design produces a superior damper as compared to the uncentered oil squeeze film damper. The air damper design produces lower bearing forces, has improved stability and will not cause damper lockup.

In summary, it appears that the future wave of dependable and reliable high-speed rolling element bearing turbochargers will consider the employment of the superior air squeeze film dampers over the existing uncentered oil squeeze film dampers currently being used with these units.

## REFERENCES

1. Alford, J. S., “**Protecting Turbomachinery from Self-Excited Rotor Whirl**”, *ASME Journal of Engineering for Power*, pp. 333 – 337, 1965
2. Barrett, L. E. and E. J. Gunter, “**Steady-State and Transient Analysis of a Squeeze Film Damper Bearing for Rotor Stability**”, *NASA CR-2548*, 1975
3. Chen, W. J., and E. J. Gunter, “**Introduction to Dynamics of Rotor-Bearing Systems**”, *Trafford Publishing*, Victoria, BC, Canada, 2005
4. Chen, W. J., Rajan, M., and H. D. Nelson, “**The Optimal Design of Squeeze Film Dampers for Flexible Rotor Systems**”, *J. Mech. Trans. Autom. Des.*, Vol 110, pp.166-174, 1988
5. Ehrich, F. F., *Handbook of Rotor Dynamics*, Krieger Publishing company, Malabar, FL., 1999
6. Gunter, E. J., “**Rotor-Bearing Stability**”, *Proc of First Turbomachinery Symposium*, pp., 119-141, 1972
7. Gunter, E. J., Barrett, L. E., and P. E. Allaire, “**Stabilization of Turbomachinery with Squeeze Film Dampers – Theory and Applications**”, *Institution of Mechanical Engineers*, 1976
8. Gunter, E. J. and W. J. Chen, “**Dynamic Analysis of a Turbocharger in Floating Bush Bearings**”, *3rd International Symposium on Stability Control of Rotating Machinery*, Cleveland, Ohio, 2005
9. Gunter, E. J. and Chen, W. J., “**Dynamic Stability and Whirl Motion of Large Diesel Engine Turbochargers in Floating Bush and Multi-Lobed Bearings**”, *Vibration Institute 34<sup>th</sup> Annual Meeting*, Oak Brook Illinois, 2010
10. Gunter, E. J. and M. P. Proctor, “**Whirl Motion of a Seal Test Rig with Squeeze – Film Dampers**”, *Vibration Institute 31<sup>st</sup> Annual Meeting*, pp. 1-12, 2007
11. Homes, R., “**Turbocharger Vibrations–Case Study**”, *Institute of Mechanical Engineering Conference on Turbochargers and Turbocharging*, pp. 91–100, 2002
12. Kirk, R. G. and E. J. Gunter, “**Effect of Support Flexibility and Damping on the Dynamic Response of the Single Mass Flexible Rotor Elastic Bearings**”, *J. Eng. Ind.*, pp. 221–232, 1972
13. Kirk, R. G., A. Alsaeed, and E. J. Gunter, “**Stability Analysis of a High-Speed Automotive Turbocharger**”, *Proceedings of ASTLE/ASME International Joint Tribology Conference*, San Antonio, Texas, 2006
14. Kirk, R. G., A. Kornhauser, J Sterling, and A. Alsaeed, “**High-Speed Turbocharger Instability**”, *ISCORMA–4*, 2007
15. Li, C. H., And Rhode, S. M., “**On the Steady-State and Dynamic Performance Characteristics of Floating Ring Bearings**”, *Trans. ASME Journal of Lubrication Technology*, Vol 103, pp. 389 – 397, 1981
17. Miller, J. K., “**TURBO-Real World High-Performance Turbocharger Systems**, Renniks Pub., Banksmeadow, NSW 2019, Australia 16.
18. Li, C. H., “**Dynamics of Rotor Bearing Systems Supported by Floating Ring Bearings**”, *Trans. ASME Journal of Lubrication*, Vol 104, pp.469-477, 1982
19. Rhode, S. M. And H. A. Ezzat, “**Analysis of Dynamically Loaded Floating-Ring Bearings for Automotive Application**”, *Trans ASME Journal of Lubrication* Vol 102, pp. 271–277, 1980
20. Tanaka, M. And Y. Hori, “**Stability Characteristics of Low they Floating Bush Bearings**”, *ASME Journal of Lubrication Technology*, Vol 94, pp. 247–259, 1972
21. Trippett, R. J. And D. F. Li,” **High-Speed Floating-Ring Bearing Test and Analysis**”, *ASME Trans.*, pp.73–81, 1983